Mascle, J., Lohmann, G.P., and Moullade, M. (Eds.), 1998
Proceedings of the Ocean Drilling Program, Scientific Results, Vol. 159

40. MIOCENE–PLIOCENE SURFACE-WATER HYDROGRAPHY OF THE EASTERN EQUATORIAL ATLANTIC[1]

Richard D. Norris[2]

ABSTRACT

Stable isotope analyses of four species of planktonic foraminifers and the benthic foraminifer, *Cibicides wuellerstorfi*, from Ocean Drilling Program Site 959 show that the Gulf of Guinea had a strong, shallow thermocline during the latest Miocene and early Pliocene prior to the first appearance of the Guinea Current at about 4.9 Ma. Gradients of $\delta^{18}O$ between the surface-water species, *Globigerinoides sacculifer*, and the thermocline species, *Neogloboquadrina dutertrei* and *Globorotalia margaritae*, were about 2‰ in the late Miocene and early Pliocene, but decreased to less than 0.5‰ in several large swings beginning about 4.9 Ma. A decreased oxygen isotope gradient in the upper ocean after 4.9 Ma is consistent with the initial establishment of the Guinea Current although several large swings in the oxygen isotope gradient shortly after this suggest that the Guinea Current did not become a permanent feature until about 4.3 Ma. The initiation of the Guinea Current in the Gulf of Guinea suggests that the Intertropical Convergence Zone (ITCZ) migrated south to near its present location at ~4.9 Ma and is in agreement with evidence for a southward shift in the ITCZ over the Pacific between 4–5 Ma. Modern hydrographic studies suggest that the position of the ITCZ modulates the strength of the North Equatorial Counter Current whose eastern extension forms the Guinea Current in the Gulf of Guinea. Notably, the interval ~4.7 to 4.3 Ma is associated with the return of a strong, shallow thermocline in the eastern Atlantic, which suggests a brief, northward drift of the ITCZ at this time and the disappearance of the Guinea Current. The Guinea Current returned to the Gulf after 4.3 Ma.

The highest sea-surface temperature (SST) occurred between ~4.4 and 5.5 Ma in the Gulf of Guinea. Warm surface waters coupled with a shallow thermocline during much of this period may have contributed to a strong West African monsoon and relatively moist conditions over sub-Saharan Africa. In contrast, the large oscillations in SST and upwelling after ~4.5 Ma may have contributed to greater variability in the monsoon and the widespread increase in terrigenous fluxes observed in deep-sea cores within the eastern Atlantic about this time.

INTRODUCTION

The structure of the surface wind field in the past is of considerable interest both because winds reflect global features like the latitudinal temperature gradient and the variability caused by changes in seasonal insolation forcing. The wind field affects the structure of the thermocline and the biological fertility of the upper ocean. Many studies have focused on glacial-interglacial variability in the wind field of the tropical Atlantic, but relatively few studies have been made of this system prior to the onset of Northern Hemisphere glaciation.

The eastern tropical Atlantic is a particularly sensitive region for studies of the tropical thermocline. The thermocline is generally shallower in the eastern Atlantic than in the western basins. Warm surface water flows to the west in the South Equatorial Current system, which piles warm water against Brazil and removes it from the West African Bight, allowing cold subsurface waters to reach the surface in the eastern Atlantic. The Gulf of Guinea is particularly sensitive to changes in the wind field over the western tropical Atlantic since the thermocline and surface-water temperatures are directly controlled by changes in the countercurrents and undercurrents produced by changes in wind stress over the western basins (Hay and Brock, 1992; Hisard and Merle, 1980; Peterson and Stramma, 1991; Verstraete, 1992). These same current systems also modulate rainfall over equatorial Africa and the strength of the African monsoon (Peterson and Stramma, 1991). The structure of the thermocline in the eastern tropical Atlantic is of considerable interest for what it reveals about the history of the tropical Atlantic wind field and climatology of the adjacent land masses. The purpose of this study is to reconstruct the vertical structure of the thermocline in the easternmost equatorial Atlantic (Fig. 1) where the response to changes in the wind field should be one of the larger in the Atlantic equatorial current system.

METHODS

Samples were taken at 20-cm intervals from Hole 959C from the top of Core 159-959C-7H to the base of Core 159-959C-11H to produce a record from ~3.5 to 6.75 Ma for four species of planktonic for-

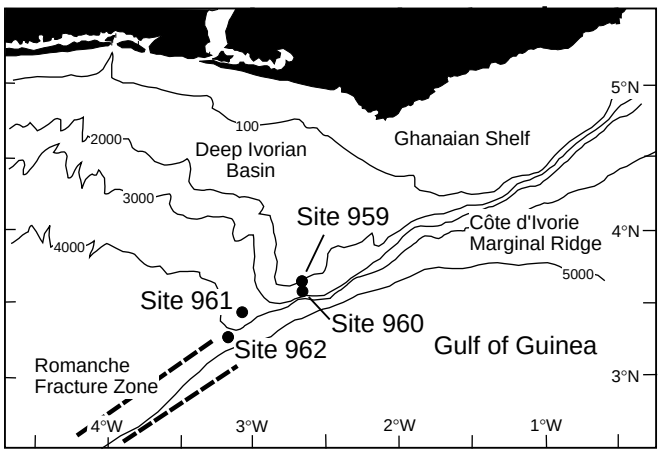

Figure 1. Location of Site 959 relative to other Leg 159 sites in the Gulf of Guinea.

[1]Mascle, J., Lohmann, G.P., and Moullade, M. (Eds.), 1998. *Proc. ODP, Sci. Results*, 159: College Station, TX (Ocean Drilling Program).

[2]MS-23, Woods Hole Oceanographic Institution, Woods Hole, MA 02543-1541, U.S.A. RNorris@whoi.edu

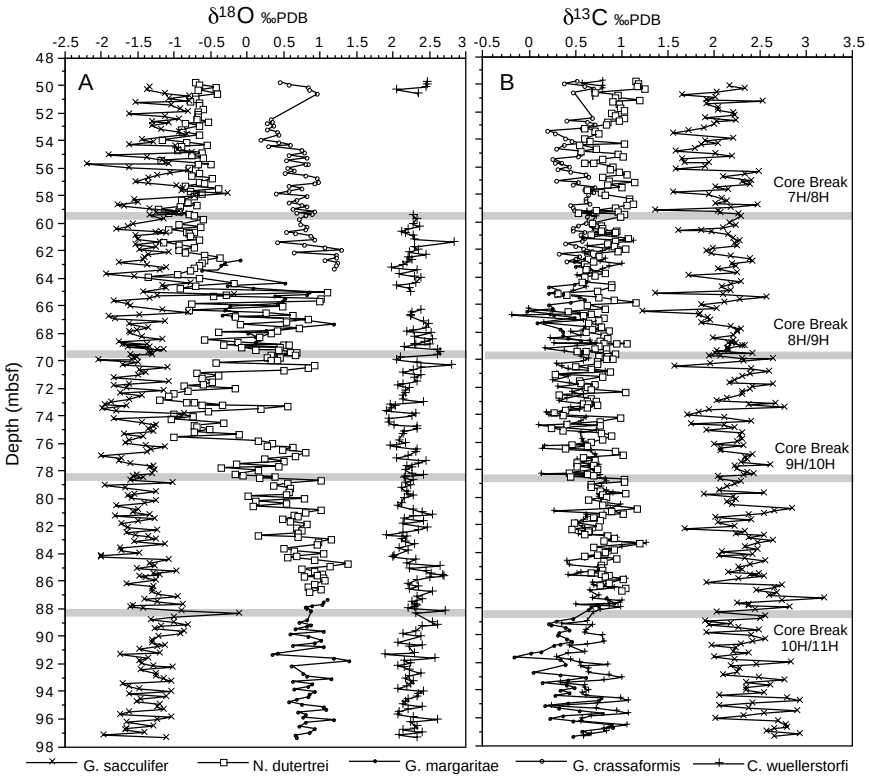

Figure 2. Stable isotope data plotted against the depth scale for Hole 959C. No correction has been made to the depth scale for sediment missing in core catchers and core breaks although the location of core breaks are indicated approximately. **A.** Records of $\delta^{18}O$ for *Globigerinoides sacculifer, Globorotalia crassaformis, Globorotalia margaritae, Neogloboquadrina dutertrei,* and *Cibicides wuellerstorfi.* Specimens of *Globorotalia cibaoensis* have been substituted for *G. margaritae* in some samples near the base of Core 159-959C-11H. The large gap in the record of *C. wuellerstorfi* between 51 and 57 mbsf was caused by loss of an entire carousel of samples in our mass spectrometer and will be replicated in the future. **B.** Records of $\delta^{13}C$ for the same taxa.

aminifers (*Globigerinoides sacculifer, Neogloboquadrina dutertrei, Globorotalia margaritae,* and *Globorotalia crassaformis*) as well as the benthic foraminifer *Cibicides wuellerstorfi* (Fig. 2). Given average sedimentation rates of 1.7–2 cm/k.y., the 20-cm sample spacing represents a temporal resolution of about 10–12 k.y. Gaps between adjacent cores were not patched by sampling overlapping sections in Holes 959A and 959B, although this could be done in the future, if need be. Instead, the volume susceptibility measurements of Holes 959A–959C were compared to estimate the magnitude of the gaps between cores in Hole 959C (Fig. 3). The amount of sediment missing between adjacent cores in Hole 959C was estimated and added to the depths recorded during drilling of this hole to create a quasi-composite depth scale. The resulting composite depth scale is applicable only to the interval studied here since I did not attempt to estimate the size of coring gaps above Core 159-959C-7H. Indeed, it has proven difficult to determine the size of these coring gaps owing to the relatively low-amplitude, monotonous volume susceptibility observed above ~47 mbsf. The depths of biostratigraphic datums used in the age model (discussed below) were also adjusted to the composite depth scale. In general, the size of coring gaps is typically ~50 cm, of which about half can be accommodated by the core catchers that were not analyzed, either for volume susceptibility or stable isotopes. However, one large coring gap of ~1.2 m has been identified between Cores 159-959C-10H and 11H (Fig. 2).

Samples were dried in a 50°C oven, soaked in a 10% Calgon solution, and washed through 64-µm sieves. The sediments contain appreciable amounts of clay and are very resistant to disaggregation in plain water. Foraminifers were picked from constant sieve fractions (300–355 µm for *G. sacculifer, G. crassaformis,* and *N. dutertrei*; 250–300 µm for *G. margaritae,* and >300 µm for *C. wuellerstorfi*). Stable isotope measurements were made with a Finnigan 252 mass spectrometer and associated single reaction vessel Kiel Device carbonate preparation system. Samples were not roasted, but were directly reacted at 90°C in phosphoric acid. Five specimens of *G. sacculifer, N. dutertrei,* and *G. crassaformis* were measured in each sample while seven specimens of *G. margaritae* and three specimens of *C. wuellerstorfi* were analyzed in samples of those species. All specimens of planktonic foraminifers were carefully checked to make sure that the inner chambers of the shells were preserved. Analytical reproducibility is about ±0.3 for $\delta^{13}C$ and ±0.08 for $\delta^{18}O$. All values were corrected to the PeeDee Belemnite (PDB) standard based on repeated analyses of National Bureau of Standards (NBS) 19, and two in-house standards: Carrara Marble and Atlantis II marine carbonate. Six standards were run during analysis of each set of 40 unknowns. Stable isotope data from Site 959 are presented in Table 1. Stable isotope results for *N. dutertrei* and *G. sacculifer* from modern Atlantic core tops are listed in Table 2.

Age Model

The age model is based on planktonic foraminiferal biostratigraphy in which datums were located to the nearest 20 cm in the same samples used for stable isotope analysis. Foraminiferal datums suggest a nearly constant long-term sedimentation rate of ~1.7 cm/k.y. from 3.12 to 5.6 Ma, followed by a slight decrease in sedimentation rate to 1 cm/k.y. in the period 5.6 to 6.4 Ma, and a renewed moderate sedimentation rate of 1.96 cm/k.y. in the late Miocene. Ages for foraminiferal datums are those given by Berggren et al. (1995).

The benthic foraminiferal stable isotope record was subsequently compared with other high resolution benthic $\delta^{13}C$ and $\delta^{18}O$ records from the tropical Atlantic (Tiedemann et al., 1994) and the tropical Pacific (Shackleton et al., 1995) to verify that the age model produced reasonable results. The 10- to 12-k.y. temporal resolution of the Hole 959C record makes it difficult to recognize any isotopic events with certainty. Prominent positive $\delta^{18}O$ excursions at 4.15 and 4.65 Ma in the Hole 959C record may correlate with the Gi16 (4.0 Ma) and NS4 (4.7 Ma) events shown in Tiedemann et al. (1994). A marked decrease in $\delta^{18}O$ in Hole 959C between 5.58 and 5.36 Ma appears to correlate with the TG14 to TG5 (~5.56–5.32 Ma) events recognized by Shackleton et al. (1995). The Messinian desiccation event

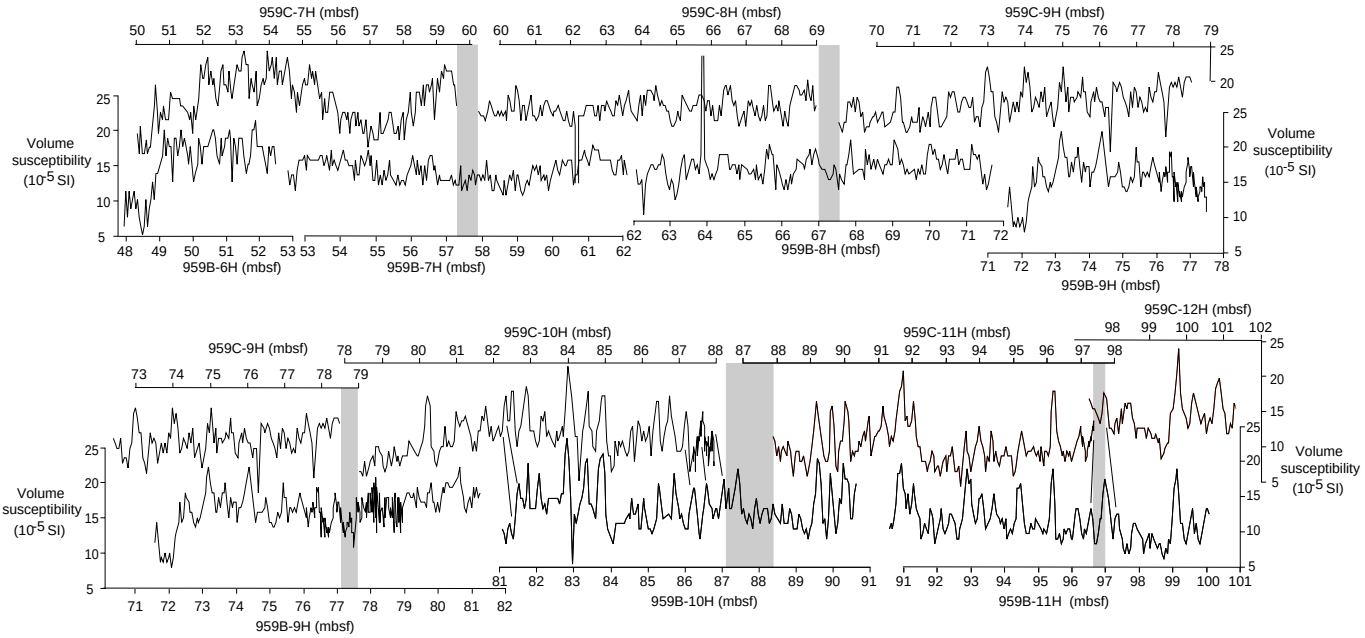

Figure 3. Volume magnetic susceptibility data plotted against depth for Holes 959A–959C showing proposed correlation between holes and estimated size of core breaks (stippled bands) in Hole 959C.

(5.32–5.8 Ma) was also used as an independent chronometer since this event is associated with widespread dissolution in Atlantic sediments. The reported ages of the Messinian desiccation are ~100 k.y. younger than the ages estimated for an interval of poor to moderate foraminifer preservation that occurs from 83.61 to 87.81 mbsf in Hole 959C and corresponds to ages of 5.45 to 5.78 Ma ± 6 k.y. The older of these dates is close to the 5.75-Ma date estimated by Shackleton et al. (1995) for an extreme glacial stage that they suggest coincides with the initial isolation of the Mediterranean Sea. All told, it appears that the Hole 959C chronology is probably offset by <100 k.y. toward older ages than the chronologies developed by Tiedemann et al. (1994) and Shackleton et al. (1995). A more refined chronology for Hole 959C awaits sampling at higher resolution to develop a less-aliased benthic foraminifer isotope record.

Isotopic and Depth-Stratification of Planktonic Foraminifers

The significance of stable isotopic variation in modern planktonic foraminifers has been the subject of many studies of material from core tops, sediment traps, and plankton tows. The $\delta^{18}O$ of foraminifers is generally regarded as being largely a product of water temperature in which a given species calcified. Salinity effects may also be important in some instances, such as marginal seas and frontal zones. A basic assumption employed in this paper is that the $\delta^{18}O$ gradient between different species of foraminifers is a measure of the temperature gradient that existed between the average depths of calcification of the species being analyzed. Ravelo and Shackleton (1995) have demonstrated that differences in the $\delta^{18}O$ of many species of planktonic foraminifers correlate well with the thermal gradient in the upper ocean. Environments with strong, permanent thermoclines, like the eastern equatorial Atlantic, produce large $\delta^{18}O$ differences between taxa growing in the surface mixed layer and deep thermocline as a reflection of the steep temperature gradient. Gradients in foraminifer $\delta^{18}O$ are smaller in the western tropical oceans where the thermocline is depressed to ~100–200 m depth and the upper ocean has relatively uniform temperature. Finally, foraminifers growing in upwelling centers with strong seasonality tend to have small $\delta^{18}O$ differences from one another because peak production of these species coincides with upwelling events when cold waters reach the surface and the vertical thermal gradient weakens.

In practice, the inference of thermocline structure is complicated by the observation that many species calcify partly in the surface ocean and partly in deeper water (Duplessy et al., 1981b; Erez and Honjo, 1981; Lohmann, 1995; Orr, 1967; Schweitzer and Lohmann, 1991). Consequently, foraminifer $\delta^{18}O$ may represent an average of the depths of calcification that is weighted by the amount of calcite grown at different temperatures. Isotopic disequilibrium may also be a problem, particularly in $\delta^{13}C$ of juvenile foraminifers and those that host algal symbionts (Berger et al., 1978; Erez, 1978; Spero and DeNiro, 1987; Spero et al., 1991).

Abundant evidence suggests that even "surface dwellers" like *Globigerinoides sacculifer* add up to ~28% of their shell calcite just prior to gametogenesis in the upper thermocline (Duplessy et al., 1981a; Duplessy et al., 1981b) and a fraction of a typical population may calcify considerably deeper than this (Lohmann, 1995). Likewise, many extant globorotaliids appear to grow most, if not all, of their chambers in the near-surface ocean, but then add up to 60% to 70% of their total shell weight in deeper water near the onset of gametogenesis (Lohmann, 1995; Norris, 1995; Orr, 1967; Schweitzer and Lohmann, 1991). The present study does not attempt to unravel the actual depths of calcification, but assumes that the weighted average depth of calcification for a given species has not changed dramatically over time. This assumption has been tested by comparing several different planktonic foraminiferal records against one another to verify that different species show similar trends. In addition, I have measured the masses of planktonic foraminifers analyzed in each sample to verify that there have not been large changes in shell mass that might be attributable to changes in the proportion of chamber calcite and secondary or "gametogenic" calcification.

For this study, *G. margaritae* was analyzed to check the isotopic history observed in *N. dutertrei*. *Neogloboquadrina dutertrei* has a relatively thick layer of "gametogenic" or secondary calcification in Leg 159 samples. Severely dissolved samples often contain what appear to be pristine specimens of *N. dutertrei* that, in fact, have had the interior chambers completely dissolved, leaving a hollow sphere of

Table 1. Stable isotope data for planktonic and benthic foraminifers from Hole 959C.

Core, section, interval (cm)	Depth (mbsf)	Composite depth (m)	Age (Ma)	Species	$\delta^{13}C$	$\delta^{18}O$	Species	$\delta^{13}C$	$\delta^{18}O$
159-959C-									
7H-1, 0	49.81	49.81	03.47				*N. dutertrei*	1.159	–0.699
7H-1, 20	50.01	50.01	03.47				*N. dutertrei*	1.182	–0.659
7H-1, 40	50.21	50.21	03.48	*G. sacculifer*	2.154	–1.345	*N. dutertrei*	1.172	–0.418
7H-1, 60	50.41	50.41	03.49	*G. sacculifer*	2.321	–1.390	*N. dutertrei*	1.250	–0.673
7H-1, 80	50.61	50.61	03.50	*G. sacculifer*	2.009	–1.134	*N. dutertrei*	0.711	–0.403
7H-1, 100	50.81	50.80	03.51	*G. sacculifer*	1.634	–0.818	*N. dutertrei*	0.955	–0.707
7H-1, 120	51.01	51.01	03.52	*G. sacculifer*	2.005	–1.095	*N. dutertrei*	0.926	–0.704
7H-1, 140	51.21	51.22	03.53	*G. sacculifer*	1.901	–0.817	*N. dutertrei*	1.193	–0.777
7H-2, 0	51.31	51.32	03.54	*G. sacculifer*	2.511	–1.550	*N. dutertrei*	0.908	–0.659
7H-2, 20	51.51	51.51	03.54	*G. sacculifer*	1.903	–1.051	*N. dutertrei*	0.974	–0.658
7H-2, 40	51.71	51.72	03.55	*G. sacculifer*	2.029	–0.926	*N. dutertrei*	0.985	–0.595
7H-2, 60	51.91	51.92	03.56	*G. sacculifer*	2.028	–0.822	*N. dutertrei*	1.030	–0.669
7H-2, 80	52.11	52.10	03.57	*G. sacculifer*	2.193	–1.639	*N. dutertrei*	0.894	–0.666
7H-2, 100	52.31	52.31	03.58	*G. sacculifer*	2.208	–1.137	*N. dutertrei*	0.938	–0.671
7H-2, 120	52.51	52.50	03.59	*G. sacculifer*	1.881	–0.950	*N. dutertrei*	1.025	–0.689
7H-2, 140	52.71	52.71	03.60	*G. sacculifer*	2.216	–1.312	*N. dutertrei*	0.978	–0.525
7H-3, 0	52.81	52.82	03.61	*G. sacculifer*	2.007	–1.085	*N. dutertrei*	0.852	–0.851
7H-3, 20	53.01	53.01	03.62	*G. sacculifer*	1.990	–1.314	*N. dutertrei*	0.836	–0.650
7H-3, 40	53.21	53.22	03.63	*G. sacculifer*	1.872	–1.190	*N. dutertrei*	0.604	–0.898
7H-3, 60	53.41	53.41	03.65	*G. sacculifer*	1.707	–0.952	*N. dutertrei*	0.710	–0.880
7H-3, 80	53.61	53.61	03.66	*G. sacculifer*	1.537	–0.850	*N. dutertrei*	0.758	–0.659
7H-3, 120	54.01	54.01	03.68	*G. sacculifer*	2.189	–1.465	*N. dutertrei*	0.596	–1.167
7H-3, 140	54.21	54.22	03.69	*G. sacculifer*	1.893	–1.308	*N. dutertrei*	0.653	–0.825
7H-4, 0	54.31	54.32	03.70	*G. sacculifer*	2.024	–1.641	*N. dutertrei*	1.032	–0.545
7H-4, 20	54.51	54.50	03.71	*G. sacculifer*	1.845	–1.004	*N. dutertrei*	0.542	–0.891
7H-4, 40	54.71	54.72	03.72	*G. sacculifer*	1.774	–0.968	*N. dutertrei*	0.721	–0.954
7H-4, 60	54.91	54.92	03.73	*G. sacculifer*	1.573	–0.778	*N. dutertrei*	0.565	–0.615
7H-4, 80	55.11	55.11	03.75	*G. sacculifer*	2.001	–1.921	*N. dutertrei*	0.967	–0.750
7H-4, 100	55.31	55.31	03.76	*G. sacculifer*	2.182	–1.388	*N. dutertrei*	1.016	–0.598
7H-4, 120	55.51	55.52	03.77	*G. sacculifer*	1.642	–1.186	*N. dutertrei*	0.800	–1.172
7H-4, 140	55.71	55.72	03.78	*G. sacculifer*	1.660	–1.098	*N. dutertrei*	0.607	–0.488
7H-5, 0	55.81	55.80	03.79	*G. sacculifer*	1.929	–2.205	*N. dutertrei*	0.702	–0.670
7H-5, 20	56.01	56.00	03.80	*G. sacculifer*	1.889	–1.627	*N. dutertrei*	0.901	–0.784
7H-5, 40	56.21	56.22	03.81	*G. sacculifer*	1.576	–0.834	*N. dutertrei*	0.878	–0.708
7H-5, 60	56.41	56.41	03.82	*G. sacculifer*	2.470	–1.079	*N. dutertrei*	0.969	–0.660
7H-5, 80	56.61	56.60	03.83	*G. sacculifer*	2.320	–1.245	*N. dutertrei*	1.061	–0.759
7H-5, 100	56.81	56.82	03.85	*G. sacculifer*	2.087	–1.376	*N. dutertrei*	0.793	–0.475
7H-5, 120	57.01	57.02	03.86	*G. sacculifer*	2.379	–1.542	*N. dutertrei*	0.863	–0.650
7H-5, 140	57.21	57.20	03.87	*G. sacculifer*	2.288	–1.376	*N. dutertrei*	1.141	–0.575
7H-6, 0	57.31	57.32	03.88	*G. sacculifer*	2.373	–0.983	*N. dutertrei*	0.855	–0.841
7H-6, 20	57.51	57.51	03.89	*G. sacculifer*	1.995	–0.906	*N. dutertrei*	0.997	–0.386
7H-6, 40	57.71	57.70	03.90	*G. sacculifer*	2.143	–0.911	*N. dutertrei*	0.634	–0.781
7H-6, 60	57.91	57.90	03.91	*G. sacculifer*	1.539	–0.283	*N. dutertrei*	0.782	–0.615
7H-6, 80	58.12	58.12	03.92	*G. sacculifer*	1.931	–0.735	*N. dutertrei*	0.821	–0.723
7H-6, 100	58.31	58.32	03.94	*G. sacculifer*	2.071	–1.559	*N. dutertrei*	1.088	–0.896
7H-6, 120	58.51	58.51	03.95	*G. sacculifer*	2.125	–1.502	*N. dutertrei*	1.086	–0.814
7H-6, 140	58.71	58.71	03.96	*G. sacculifer*	1.995	–1.782	*N. dutertrei*	1.131	–0.693
7H-7, 0	58.81	58.82	03.97	*G. sacculifer*	2.456	–1.699	*N. dutertrei*	1.056	–0.907
7H-7, 20	59.01	59.01	03.98	*G. sacculifer*	2.160	–1.351	*N. dutertrei*	0.926	–1.221
7H-7, 40	59.21	59.21	03.99	*G. sacculifer*	1.352	–0.945	*N. dutertrei*	0.721	–0.924
7H-7, 80	59.31	59.31	03.99	*G. sacculifer*	2.023	–1.267	*N. dutertrei*	0.956	–1.071
7H-7, 60	59.41	59.42	04.00	*G. sacculifer*	2.056	–0.887	*N. dutertrei*	0.537	–0.800
8H-1, 20	59.51	60.10	04.04	*G. sacculifer*	2.254	–1.359	*N. dutertrei*	1.035	–0.723
8H-1, 40	59.71	60.31	04.05	*G. sacculifer*	2.280	–1.166	*N. dutertrei*	0.985	–0.592
8H-1, 80	60.11	60.71	04.08	*G. sacculifer*	2.151	–1.581	*N. dutertrei*	0.677	–0.930
8H-1, 100	60.31	60.91	04.09	*G. sacculifer*	2.217	–1.650	*N. dutertrei*	0.780	–0.640
8H-1, 120	60.51	61.12	04.10	*G. sacculifer*	2.075	–1.808	*N. dutertrei*	0.793	–1.071
8H-1, 140	60.71	61.31	04.11	*G. sacculifer*	1.593	–1.197	*N. dutertrei*	0.780	–0.826
8H-1, 140	60.71	61.31	04.11	*G. sacculifer*	1.847	–1.264	*N. dutertrei*	0.943	–0.717
8H-2, 0	60.81	61.40	04.12	*G. sacculifer*	1.960	–1.117	*N. dutertrei*	0.938	–0.790
8H-2, 20	61.01	61.61	04.13	*G. sacculifer*	2.143	–1.548	*N. dutertrei*	0.666	–0.767
8H-2, 40	61.21	61.82	04.14	*G. sacculifer*	2.198	–1.515	*N. dutertrei*	1.071	–0.658
8H-2, 60	61.41	62.02	04.15	*G. sacculifer*	2.265	–1.219	*N. dutertrei*	0.928	–1.138
8H-2, 80	61.61	62.21	04.17	*G. sacculifer*	2.211	–1.552	*N. dutertrei*	0.852	–0.939
8H-2, 100	61.81	62.41	04.18	*G. sacculifer*	2.229	–1.259	*N. dutertrei*	0.912	–0.717
8H-2, 120	62.01	62.61	04.19	*G. sacculifer*	1.965	–1.494	*N. dutertrei*	1.040	–0.935
8H-2, 140	62.21	62.80	04.20	*G. sacculifer*	1.908	–1.091	*N. dutertrei*	0.961	–0.839
8H-3, 0	62.31	62.92	04.21	*G. sacculifer*	1.953	–1.366	*N. dutertrei*	0.697	–0.590
8H-3, 20	62.51	63.12	04.22	*G. sacculifer*	2.166	–1.424	*N. dutertrei*	0.758	–0.372
8H-3, 40	62.71	63.32	04.23	*G. sacculifer*	2.366	–1.433	*N. dutertrei*	0.645	–0.575
8H-3, 60	62.91	63.52	04.24	*G. sacculifer*	2.403	–1.765	*N. dutertrei*	0.703	–0.614
8H-3, 80	63.11	63.72	04.25	*G. sacculifer*	2.179	–1.391	*N. dutertrei*	0.596	–0.660
8H-3, 100	63.31	63.92	04.26	*G. sacculifer*	2.220	–1.119		0.624	–0.718
8H-3, 120	63.51	64.12	04.27	*G. sacculifer*	2.025	–1.213	*N. dutertrei*	0.610	–0.773
8H-3, 140	63.71	64.32	04.28	*G. sacculifer*	2.240	–1.946	*N. dutertrei*	0.821	–0.944
8H-4, 0	63.91	64.52	04.29	*G. sacculifer*	1.712	–1.566	*N. dutertrei*	0.711	–1.346
8H-4, 20	64.01	64.61	04.29	*G. sacculifer*			*N. dutertrei*	0.601	–0.644
8H-4, 60	64.41	65.02	04.32	*G. sacculifer*	2.274	–0.787	*N. dutertrei*	0.574	–0.174
8H-4, 80	64.61	65.22	04.33	*G. sacculifer*	2.170	–1.178	*N. dutertrei*	0.885	–0.708
8H-4, 100	64.81	65.42	04.34	*G. sacculifer*	2.072	–1.117	*N. dutertrei*	0.887	–0.908
8H-4, 120	65.01	65.62	04.35	*G. sacculifer*	2.169	–1.436	*N. dutertrei*	0.732	1.103
8H-4, 140	65.21	65.82	04.36	*G. sacculifer*	1.343	–0.191	*N. dutertrei*	0.312	–0.284
8H-5, 0	65.31	65.92	04.36	*G. sacculifer*	2.087	–1.242	*N. dutertrei*	0.405	–0.464
8H-5, 20	65.51	66.12	04.37	*G. sacculifer*	2.546	–1.349	*N. dutertrei*	0.748	1.018
8H-5, 40	65.71	66.32	04.38	*G. sacculifer*	2.262	–1.835	*N. dutertrei*	0.920	0.987
8H-5, 60	65.91	66.52	04.39	*G. sacculifer*	2.092	–1.652	*N. dutertrei*	1.156	–0.764
8H-5, 80	66.11	66.72	04.40	*G. sacculifer*	1.841	–1.623	*N. dutertrei*	0.624	0.478
8H-5, 100	66.31	66.92	04.42	*G. sacculifer*	2.019	–1.169	*N. dutertrei*	0.823	–0.792
8H-5, 120	66.51	67.12	04.43	*G. sacculifer*	1.210	–0.831	*N. dutertrei*	0.425	0.266

Table 1 (continued).

Core, section, interval (cm)	Depth (mbsf)	Composite depth (m)	Age (Ma)	Species	$\delta^{13}C$	$\delta^{18}O$	Species	$\delta^{13}C$	$\delta^{18}O$
159-959C-									
8H-5, 140	66.71	67.32	04.44	*G. sacculifer*	1.826	–1.501	*N. dutertrei*	0.663	0.629
8H-6, 0	66.81	67.41	04.44	*G. sacculifer*	1.821	–1.905	*N. dutertrei*	0.589	–0.168
8H-6, 20	67.01	67.61	04.45	*G. sacculifer*	1.911	–1.825	*N. dutertrei*	0.805	0.836
8H-6, 40	67.21	67.81	04.46	*G. sacculifer*	1.948	–1.143	*N. dutertrei*	0.750	0.547
8H-6, 60	67.41	68.01	04.47	*G. sacculifer*	1.842	–1.636	*N. dutertrei*	0.640	–0.097
8H-6, 80	67.61	68.21	04.48	*G. sacculifer*	2.164	–1.372	*N. dutertrei*	0.777	0.711
8H-6, 100	67.81	68.41	04.49	*G. sacculifer*	2.280	–1.526	*N. dutertrei*	0.681	0.416
8H-6, 100	67.91	68.50	04.50	*G. sacculifer*	2.236	–1.632	*N. dutertrei*	0.861	–0.390
8H-6, 120	68.01	68.61	04.50	*G. sacculifer*	2.227	–1.618	*N. dutertrei*	0.609	0.324
8H-7, 0	68.31	68.90	04.52	*G. sacculifer*	2.196	–1.450	*N. dutertrei*	0.813	0.167
8H-7, 20	68.51	69.10	04.53	*G. sacculifer*	1.966	–1.174	*N. dutertrei*	0.851	–0.574
8H-7, 40	68.71	69.30	04.54	*G. sacculifer*	2.188	–1.778	*N. dutertrei*	0.760	–0.124
9H-1, 0	68.81	70.02	04.58	*G. sacculifer*	2.135	–1.384	*N. dutertrei*	0.806	0.508
9H-1, 0	68.81	70.02	04.58	*G. sacculifer*	2.218	–1.714	*N. dutertrei*	0.948	0.567
8H-7, 60	68.91	70.11	04.58	*G. sacculifer*	2.176	–1.686	*N. dutertrei*	1.058	–0.323
9H-1, 20	69.01	70.22	04.59	*G. sacculifer*	2.311	–1.359	*N. dutertrei*	0.748	0.452
9H-1, 20	69.01	70.22	04.59	*G. sacculifer*	2.286	–1.655	*N. dutertrei*	0.748	–0.069
9H-1, 40	69.21	70.41	04.60	*G. sacculifer*	2.134	–1.242	*N. dutertrei*	0.710	0.111
9H-1, 40	69.21	70.41	04.60	*G. sacculifer*	2.125	–1.165	*N. dutertrei*	0.839	0.439
9H-1, 60	69.41	70.62	04.61	*G. sacculifer*	2.141	–1.367	*N. dutertrei*	0.621	0.583
9H-1, 60	69.41	70.62	04.61	*G. sacculifer*	2.006	–1.343	*N. dutertrei*	0.513	0.677
9H-1, 80	69.61	70.81	04.62	*G. sacculifer*	2.394	–1.315	*N. dutertrei*	0.933	0.334
9H-1, 80	69.61	70.81	04.62	*G. sacculifer*	2.005	–1.618	*N. dutertrei*	0.829	0.663
9H-1, 100	69.81	71.01	04.63	*G. sacculifer*	1.923	–1.533	*N. dutertrei*	0.847	0.285
9H-1, 100	69.81	71.01	04.63	*G. sacculifer*	2.053	–1.529	*N. dutertrei*	0.747	0.447
9H-1, 120	70.01	71.22	04.64	*G. sacculifer*	2.287	–1.593	*N. dutertrei*	0.829	0.324
9H-1, 120	70.01	71.22	04.64	*G. sacculifer*	2.626	–2.051	*N. dutertrei*	0.902	0.409
9H-1, 140	70.21	71.41	04.65	*G. sacculifer*	2.309	–1.506	*N. dutertrei*	0.739	–0.430
9H-2, 0	70.31	71.52	04.65	*G. sacculifer*	1.949	–1.721	*N. dutertrei*	0.734	0.924
9H-2, 20	70.51	71.71	04.66	*G. sacculifer*	1.551	–1.100	*N. dutertrei*	0.505	0.834
9H-2, 40	70.71	71.92	04.68	*G. sacculifer*	2.385	–1.489	*N. dutertrei*	0.675	0.508
9H-2, 60	70.91	72.10	04.68	*G. sacculifer*	2.582	–1.408	*N. dutertrei*	0.878	–0.692
9H-2, 80	71.11	72.30	04.70	*G. sacculifer*	2.375	–1.518	*N. dutertrei*	0.286	–0.386
9H-2, 100	71.31	72.50	04.71	*G. sacculifer*	2.283	–1.845	*N. dutertrei*	0.796	–0.622
9H-2, 120	71.51	72.72	04.72	*G. sacculifer*	2.212	–1.085	*N. dutertrei*	0.544	–0.478
9H-2, 140	71.71	72.90	04.73	*G. sacculifer*	2.144	–1.634	*N. dutertrei*	0.552	–0.603
9H-3, 0	71.81	73.02	04.73	*G. sacculifer*	2.626	–1.847	*N. dutertrei*	0.709	–0.863
9H-3, 20	72.01	73.21	04.74	*G. sacculifer*	2.405	–1.671	*N. dutertrei*	0.622	–0.167
9H-3, 40	72.21	73.42	04.75	*G. sacculifer*	2.377	–1.167	*N. dutertrei*	0.675	–0.808
9H-3, 60	72.41	73.61	04.76	*G. sacculifer*	2.294	–1.760	*N. dutertrei*	1.049	-1.003
9H-3, 80	72.61	73.82	04.77	*G. sacculifer*	2.287	–1.460	*N. dutertrei*	0.330	–1.076
9H-3, 100	72.81	74.02	04.78	*G. sacculifer*	2.125	–1.641	*N. dutertrei*	0.672	–1.191
9H-3, 120	73.01	74.21	04.79				*N. dutertrei*	0.728	–0.819
9H-3, 120	73.01	74.21	04.79	*G. sacculifer*	2.014	–1.884	*N. dutertrei*	0.628	–0.720
9H-3, 140	73.21	74.41	04.81				*N. dutertrei*	0.584	–0.334
9H-3, 140	73.21	74.41	04.81	*G. sacculifer*	2.649	–1.973	*N. dutertrei*	0.640	–0.622
9H-4, 0	73.31	74.52	04.81	*G. sacculifer*	2.362	–1.676	*N. dutertrei*	0.741	0.564
9H-4, 20	73.51	74.71	04.82	*G. sacculifer*	2.744	–1.997	*N. dutertrei*	0.628	0.197
9H-4, 40	73.71	74.90	04.83	*G. sacculifer*	1.935	–1.810	*N. dutertrei*	0.393	–0.524
9H-4, 60	73.91	75.11	04.84	*G. sacculifer*	1.815	–0.883	*N. dutertrei*	0.268	–1.003
9H-4, 80	74.11	75.30	04.85	*G. sacculifer*	1.689	–0.920	*N. dutertrei*	0.370	–0.732
9H-4, 100	74.31	75.50	04.86	*G. sacculifer*	2.097	–1.843	*N. dutertrei*	0.991	–1.045
9H-4, 120	74.51	75.72	04.87	*G. sacculifer*	2.392	–1.465	*N. dutertrei*	0.771	–0.312
9H-4, 140	74.71	75.91	04.88	*G. sacculifer*	1.742	–1.270	*N. dutertrei*	0.407	–0.722
9H-5, 0	74.81	76.02	04.89	*G. sacculifer*	2.101	–1.303	*N. dutertrei*	0.764	–0.687
9H-5, 20	75.01	76.21	04.90	*G. sacculifer*	2.208	–1.362	*N. dutertrei*	0.239	–0.519
9H-5, 40	75.21	76.42	04.91	*G. sacculifer*	1.903	–1.305	*N. dutertrei*	0.369	–0.723
9H-5, 60	75.41	76.60	04.92	*G. sacculifer*	2.289	–1.700	*N. dutertrei*	0.778	–0.102
9H-5, 80	75.61	76.80	04.93	*G. sacculifer*	2.258	–1.435	*N. dutertrei*	0.893	–0.999
9H-5, 100	75.81	77.00	04.94	*G. sacculifer*	2.293	–1.637	*N. dutertrei*	0.797	0.151
9H-5, 120	76.01	77.22	04.95	*G. sacculifer*	2.230	–1.678	*N. dutertrei*	0.673	0.349
9H-5, 140	76.21	77.41	04.96	*G. sacculifer*	1.987	–1.405	*N. dutertrei*	0.463	0.272
9H-6, 0	76.31	77.50	04.97	*G. sacculifer*	2.303	–1.148	*N. dutertrei*	0.626	0.628
9H-6, 20	76.51	77.71	04.98	*G. sacculifer*	2.057	–1.332	*N. dutertrei*	0.391	0.482
9H-6, 40	76.71	77.91	04.99	*G. sacculifer*	2.051	–1.395	*N. dutertrei*	0.938	0.810
9H-6, 60	76.91	78.12	05.00	*G. sacculifer*	2.404	–2.017	*N. dutertrei*	1.018	0.659
9H-6, 80	77.11	78.31	05.01	*G. sacculifer*	2.319	–1.741	*N. dutertrei*	0.590	0.244
9H-6, 100	77.31	78.52	05.02	*G. sacculifer*	2.349	–1.771	*N. dutertrei*	0.706	0.500
9H-6, 120	77.51	78.72	05.03	*G. sacculifer*	2.279	–1.621	*N. dutertrei*	0.514	–0.136
9H-6, 140	77.71	78.92	05.04	*G. sacculifer*	2.594	–1.299	*N. dutertrei*	0.696	0.429
9H-7, 0	77.81	79.02	05.05	*G. sacculifer*	2.200	–1.347	*N. dutertrei*	0.515	–0.357
9H-7, 20	78.01	79.21	05.06	*G. sacculifer*	2.229	–1.275	*N. dutertrei*	0.734	0.156
9H-7, 40	78.21	79.42	05.07	*G. sacculifer*	2.339	–1.310	*N. dutertrei*	0.428	–0.155
10H-1, 0	78.31	79.52	05.07	*G. sacculifer*	2.420	–1.529	*N. dutertrei*	0.628	–0.060
9H-7, 60	78.41	80.11	05.10	*G. sacculifer*	2.299	–1.589	*N. dutertrei*	0.691	0.377
10H-1, 20	78.51	80.21	05.11	*G. sacculifer*	2.030	–1.438	*N. dutertrei*	0.444	0.176
10H-1, 40	78.71	80.42	05.12	*G. sacculifer*	2.056	–1.618	*N. dutertrei*	1.030	1.007
10H-1, 60	78.91	80.60	05.13	*G. sacculifer*	2.279	–1.034	*N. dutertrei*	1.033	0.550
10H-1, 80	79.11	80.82	05.14	*G. sacculifer*	2.202	–1.974	*N. dutertrei*	0.665	0.367
10H-1, 100	79.31	81.01	05.15	*G. sacculifer*	2.124	–1.681	*N. dutertrei*	0.668	0.589
10H-1, 120	79.51	81.22	05.16	*G. sacculifer*	2.043	–1.268	*N. dutertrei*	0.764	0.573
10H-1, 140	79.71	81.42	05.17	*G. sacculifer*	2.524	–1.556	*N. dutertrei*	1.048	0.545
10H-2, 0	79.81	81.52	05.18	*G. sacculifer*	1.878	–1.656	*N. dutertrei*	0.796	0.015
10H-2, 20	80.01	81.71	05.19	*G. sacculifer*	2.188	–1.599	*N. dutertrei*	0.830	0.782
10H-2, 40	80.21	81.92	05.20	*G. sacculifer*	2.224	–1.268	*N. dutertrei*	0.636	0.126
10H-2, 60	80.41	82.10	05.21	*G. sacculifer*	2.128	–1.418	*N. dutertrei*	0.811	0.534
10H-2, 80	80.61	82.30	05.22	*G. sacculifer*	2.180	–1.801	*N. dutertrei*	0.796	0.092
10H-2, 100	80.81	82.52	05.24	*G. sacculifer*	2.829	–1.515	*N. dutertrei*	1.164	1.011
10H-2, 120	81.01	82.71	05.25	*G. sacculifer*	2.634	–1.574	*N. dutertrei*	0.890	0.810

Table 1 (continued).

Core, section, interval (cm)	Depth (mbsf)	Composite depth (m)	Age (Ma)	Species	$\delta^{13}C$	$\delta^{18}O$	Species	$\delta^{13}C$	$\delta^{18}O$
159-959C-									
10H-2, 140	81.21	82.92	05.27	*G. sacculifer*	2.522	–1.355	*N. dutertrei*	1.012	0.638
10H-3, 0	81.31	83.02	05.28	*G. sacculifer*	2.364	–1.831	*N. dutertrei*	0.797	0.697
10H-3, 20	81.51	83.21	05.29	*G. sacculifer*	1.993	–1.275	*N. dutertrei*	0.692	0.495
10H-3, 40	81.71	83.42	05.31	*G. sacculifer*	2.383	–1.510	*N. dutertrei*	0.763	0.589
10H-3, 60	81.91	83.60	05.32	*G. sacculifer*	2.028	–1.731	*N. dutertrei*	0.491	0.811
10H-3, 80	82.11	83.82	05.33	*G. sacculifer*	2.211	–1.653	*N. dutertrei*	0.753	0.672
10H-3, 100	82.31	84.02	05.35	*G. sacculifer*	1.664	–1.254	*N. dutertrei*	0.466	0.747
10H-3, 120	82.51	84.21	05.36	*G. sacculifer*	2.313	–1.675	*N. dutertrei*	0.636	0.699
10H-3, 140	82.71	84.42	05.38	*G. sacculifer*	2.221	–1.549	*N. dutertrei*	0.605	0.149
10H-4, 0	82.81	84.52	05.39	*G. sacculifer*	2.518	–1.365	*N. dutertrei*	0.848	0.697
10H-4, 20	83.01	84.71	05.40	*G. sacculifer*	2.360	–1.267	*N. dutertrei*	0.921	1.154
10H-4, 40	83.21	84.92	05.42	*G. sacculifer*	2.622	–1.565	*N. dutertrei*	0.812	0.978
10H-4, 60	83.41	85.10	05.43	*G. sacculifer*	2.451	–1.144	*N. dutertrei*	1.197	0.961
10H-4, 80	83.61	85.32	05.45	*G. sacculifer*	2.315	–1.761	*N. dutertrei*	0.702	0.508
10H-4, 100	83.81	85.52	05.46	*G. sacculifer*	2.451	–1.732	*N. dutertrei*	0.923	0.640
10H-4, 120	84.01	85.72	05.48	*G. sacculifer*	2.070	–1.487	*N. dutertrei*	0.826	1.055
10H-4, 140	84.21	85.91	05.49	*G. sacculifer*	2.399	–2.021	*N. dutertrei*	0.744	0.673
10H-5, 0	84.31	86.01	05.50	*G. sacculifer*	2.046	–2.013	*N. dutertrei*	0.596	0.565
10H-5, 20	84.51	86.21	05.51	*G. sacculifer*	2.320	–1.092	*N. dutertrei*	0.945	0.927
10H-5, 40	84.71	86.41	05.53	*G. sacculifer*	2.544	–1.344	*N. dutertrei*	0.804	1.386
10H-5, 60	84.91	86.62	05.54	*G. sacculifer*	2.366	–1.275	*N. dutertrei*	0.777	1.131
10H-5, 80	85.11	86.82	05.56	*G. sacculifer*	2.245	–1.521	*N. dutertrei*	0.783	0.746
10H-5, 100	85.31	87.02	05.57	*G. sacculifer*	2.292	–0.990	*N. dutertrei*	0.793	0.917
10H-5, 120	85.51	87.22	05.59	*G. sacculifer*	2.140	–1.303	*N. dutertrei*	0.663	1.021
10H-5, 130	85.61	87.31	05.59	*G. sacculifer*	2.469	–1.216	*N. dutertrei*	0.784	0.965
10H-5, 140	85.71	87.41	05.60	*G. sacculifer*	2.368	–1.497	*N. dutertrei*	0.863	0.786
10H-6, 0	85.81	87.52	05.61	*G. sacculifer*	2.521	–1.413	*N. dutertrei*	0.820	1.040
10H-6, 20	86.01	87.71	05.62	*G. sacculifer*	2.243	–1.259	*N. dutertrei*	1.019	1.071
10H-6, 40	86.21	87.92	05.64	*G. sacculifer*	1.902	–1.666	*N. dutertrei*	0.859	0.933
10H-6, 60	86.41	88.10	05.66	*G. sacculifer*	2.715	–1.304	*N. dutertrei*	0.763	0.832
10H-6, 80	86.61	88.32	05.68	*G. sacculifer*	2.637	–1.312	*N. dutertrei*	1.050	1.007
10H-6, 100	86.81	88.52	05.69	*G. sacculifer*	2.438	–1.319	*N. dutertrei*	0.995	0.858
10H-6, 120	87.01	88.72	05.71	*G. sacculifer*	2.656	–1.226			
10H-6, 140	87.21	88.90	05.73	*G. sacculifer*	2.586	–0.969			
10H-7, 0	87.31	89.02	05.74	*G. sacculifer*	3.170	–1.420			
10H-7, 20	87.51	89.21	05.75	*G. sacculifer*	2.714	–1.251			
10H-7, 40	87.71	89.41	05.77	*G. sacculifer*	2.227	–0.896			
11H-1, 0	87.81	89.52	05.78	*G. sacculifer*	2.360	–1.585			
10H-7, 60	87.91	90.82	05.89	*G. sacculifer*	2.357	–1.609			
11H-1, 20	88.01	90.91	05.89	*G. sacculifer*	2.797	–1.447			
11H-1, 40	88.21	91.12	05.91	*G. sacculifer*	2.428	–0.914			
11H-1, 60	88.41	91.31	05.93	*G. sacculifer*	2.010	–0.131			
11H-1, 80	88.61	91.52	05.95	*G. sacculifer*	2.542	–1.021			
11H-1, 100	88.81	91.71	05.96	*G. sacculifer*	2.489	–1.329			
11H-1, 120	89.01	91.92	05.98	*G. sacculifer*	1.882	–1.021			
11H-1, 140	89.21	92.11	06.00	*G. sacculifer*	2.170	–0.832			
11H-2, 0	89.31	92.22	06.01	*G. sacculifer*	1.927	–1.203			
11H-2, 20	89.51	92.41	06.02	*G. sacculifer*	2.243	–1.285			
11H-2, 40	89.71	92.62	06.04	*G. sacculifer*	2.462	–0.872			
11H-2, 60	89.91	92.81	06.05	*G. sacculifer*	1.897	–0.926			
11H-2, 80	90.11	93.00	06.07	*G. sacculifer*	2.383	–1.238			
11H-2, 100	90.31	93.20	06.09	*G. sacculifer*	2.544	–1.321			
11H-2, 120	90.51	93.41	06.11	*G. sacculifer*	2.400	–1.324			
11H-2, 140	90.71	93.62	06.12	*G. sacculifer*	2.281	–1.151			
11H-3, 0	90.81	93.72	06.13	*G. sacculifer*	1.951	–1.254			
11H-3, 20	91.01	93.92	06.15	*G. sacculifer*	2.226	–1.488			
11H-3, 40	91.21	94.12	06.17	*G. sacculifer*	2.190	–1.217			
11H-3, 60	91.41	94.30	06.18	*G. sacculifer*	2.353	–1.760			
11H-3, 80	91.61	94.52	06.20	*G. sacculifer*	1.987	–1.362			
11H-3, 100	91.81	94.71	06.22	*G. sacculifer*	2.202	–1.489			
11H-3, 120	92.01	94.92	06.23	*G. sacculifer*	2.820	–1.455			
11H-3, 140	92.21	95.11	06.25	*G. sacculifer*	2.444	–1.308			
11H-4, 0	92.31	95.22	06.26	*G. sacculifer*	2.171	–1.038			
11H-4, 20	92.51	95.41	06.27	*G. sacculifer*	2.261	–1.475			
11H-4, 40	92.71	95.62	06.29	*G. sacculifer*	2.233	–1.260			
11H-4, 60	92.91	95.80	06.31	*G. sacculifer*	2.078	–1.271			
11H-4, 80	93.11	96.02	06.33	*G. sacculifer*	2.468	–1.165			
11H-4, 100	93.31	96.22	06.34	*G. sacculifer*	2.743	–1.053			
11H-4, 120	93.51	96.41	06.36	*G. sacculifer*	2.330	–1.720			
11H-4, 140	93.71	96.62	06.38	*G. sacculifer*	2.592	–1.632			
11H-5, 0	93.81	96.72	06.38	*G. sacculifer*	2.326	–1.490			
11H-5, 20	94.01	96.91	06.40	*G. sacculifer*	2.324	–1.048			
11H-5, 40	94.21	97.12	06.42	*G. sacculifer*	2.518	–1.625			
11H-5, 60	94.41	97.30	06.43	*G. sacculifer*	2.043	–1.120			
11H-5, 80	94.61	97.50	06.45	*G. sacculifer*	2.769	–1.467			
11H-5, 100	94.81	97.71	06.47	*G. sacculifer*	2.911	–1.533			
11H-5, 120	95.01	97.90	06.48	*G. sacculifer*	2.394	–1.210			
11H-5, 140	95.21	98.11	06.50	*G. sacculifer*	2.042	–1.243			
11H-6, 0	95.31	98.22	06.51	*G. sacculifer*	2.358	–1.161			
11H-6, 20	95.51	98.41	06.53	*G. sacculifer*	2.887	–1.640			
11H-6, 40	95.71	98.60	06.54	*G. sacculifer*	2.531	–1.759			
11H-6, 60	95.91	98.81	06.56	*G. sacculifer*	2.300	–1.060			
11H-6, 80	96.11	99.01	06.58	*G. sacculifer*	2.005	–1.247			
11H-6, 100	96.31	99.21	06.59	*G. sacculifer*	2.680	–1.661			
11H-6, 120	96.51	99.42	06.61	*G. sacculifer*	2.755	–1.293			
11H-6, 140	96.71	99.60	06.63	*G. sacculifer*	2.767	–1.667			
11H-7, 0	96.81	99.72	06.64	*G. sacculifer*	2.636	–1.684			
11H-7, 20	97.01	99.91	06.65	*G. sacculifer*	2.547	–1.427			

Table 1 (continued).

Core, section, interval (cm)	Depth (mbsf)	Composite depth (m)	Age (Ma)	Species	$\delta^{13}C$	$\delta^{18}O$	Species	$\delta^{13}C$	$\delta^{18}O$
159-959C-									
11H-7, 40	97.21	100.12	06.67	*G. sacculifer*	2.913	–1.987			
11H-7, 60	97.41	100.32	06.69	*G. sacculifer*	2.630	–1.118			
7H-1, 0	49.81	49.81	03.47	*C. wuellerstorfi*	0.777	2.451			
7H-1, 20	50.01	50.01	03.47	*C. wuellerstorfi*	0.557	2.448			
7H-1, 40	50.21	50.21	03.48	*C. wuellerstorfi*	0.775	2.431			
7H-1, 60	50.41	50.41	03.49	*C. wuellerstorfi*	0.781	2.023			
7H-1, 80	50.61	50.61	03.50	*C. wuellerstorfi*	0.680	2.329			
8H-1, 20	59.51	60.10	04.04	*C. wuellerstorfi*	0.614	2.251			
8H-1, 40	59.71	60.31	04.05	*C. wuellerstorfi*	0.706	2.310			
8H-1, 80	60.11	60.71	04.08	*C. wuellerstorfi*	0.650	2.252			
8H-1, 100	60.31	60.91	04.09	*C. wuellerstorfi*	0.652	2.347			
8H-1, 120	60.51	61.12	04.10	*C. wuellerstorfi*	0.676	2.184			
8H-1, 140	60.71	61.31	04.11	*C. wuellerstorfi*	0.806	2.099			
8H-2, 0	60.81	61.40	04.12	*C. wuellerstorfi*	0.684	2.156			
8H-2, 20	61.01	61.61	04.13	*C. wuellerstorfi*	0.876	2.249			
8H-2, 40	61.21	61.82	04.14	*C. wuellerstorfi*	0.562	2.274			
8H-2, 60	61.41	62.02	04.15	*C. wuellerstorfi*	1.119	2.809			
8H-2, 100	61.81	62.41	04.18	*C. wuellerstorfi*	0.614	2.266			
8H-2, 120	62.01	62.61	04.19	*C. wuellerstorfi*	0.849	2.322			
8H-2, 140	62.21	62.80	04.20	*C. wuellerstorfi*	0.787	2.210			
8H-3, 0	62.31	62.92	04.21	*C. wuellerstorfi*	0.586	2.439			
8H-3, 20	62.51	63.12	04.22	*C. wuellerstorfi*	0.704	2.182			
8H-3, 40	62.71	63.32	04.23	*C. wuellerstorfi*	0.814	2.237	*G. margaritae*	0.609	–0.149
8H-3, 60	62.91	63.52	04.24	*C. wuellerstorfi*	0.750	2.170	*G. margaritae*	0.466	–0.454
8H-3, 80	63.11	63.72	04.25	*C. wuellerstorfi*	0.989	2.117	*G. margaritae*	0.622	–0.406
8H-3, 100	63.31	63.92	04.26	*C. wuellerstorfi*	0.851	1.960	*G. margaritae*	0.646	–0.699
8H-3, 120	63.51	64.12	04.27	*C. wuellerstorfi*	0.780	2.313			
8H-3, 140	63.71	64.32	04.28	*C. wuellerstorfi*	0.668	2.058			
8H-4, 0	63.91	64.52	04.29	*C. wuellerstorfi*	0.502	2.269			
8H-4, 20	64.01	64.61	04.29	*C. wuellerstorfi*	0.574	2.366			
8H-4, 60	64.41	65.02	04.32	*C. wuellerstorfi*	0.613	2.290	*G. margaritae*	0.594	0.462
8H-4, 80	64.61	65.22	04.33	*C. wuellerstorfi*	0.574	2.029	*G. margaritae*	0.464	–0.444
8H-4, 100	64.81	65.42	04.34	*C. wuellerstorfi*	0.597	2.202	*G. margaritae*	0.222	0.011
8H-4, 120	65.01	65.62	04.35	*C. wuellerstorfi*	0.464	2.221	*G. margaritae*	0.307	0.742
8H-4, 140	65.21	65.82	04.36				*G. margaritae*	0.223	0.771
8H-5, 0	65.31	65.92	04.36				*G. margaritae*	0.342	0.258
8H-5, 20	65.51	66.12	04.37				*G. margaritae*	0.559	0.495
8H-5, 40	65.71	66.32	04.38				*G. margaritae*	0.589	0.390
8H-5, 60	65.91	66.52	04.39				*G. margaritae*	0.462	0.356
8H-5, 80	66.11	66.72	04.40				*G. margaritae*	0.194	–0.380
8H-5, 100	66.31	66.92	04.42	*C. wuellerstorfi*	–0.018	2.359	*G. margaritae*	0.225	–0.479
8H-5, 120	66.51	67.12	04.43	*C. wuellerstorfi*	0.238	2.244	*G. margaritae*	–0.018	–0.198
8H-5, 140	66.71	67.32	04.44	*C. wuellerstorfi*	0.531	2.227	*G. margaritae*	0.228	–0.399
8H-6, 0	66.81	67.41	04.44	*C. wuellerstorfi*	–0.199	2.218	*G. margaritae*	0.246	–0.308
8H-6, 20	67.01	67.61	04.45				*G. margaritae*	0.493	0.568
8H-6, 40	67.21	67.81	04.46	*C. wuellerstorfi*	0.573	2.393			
8H-6, 60	67.41	68.01	04.47	*C. wuellerstorfi*	0.138	2.460	*G. margaritae*	0.058	1.030
8H-6, 80	67.61	68.21	04.48	*C. wuellerstorfi*	0.601	2.427			
8H-6, 100	67.81	68.41	04.49	*C. wuellerstorfi*	0.573	2.257	*G. margaritae*	0.351	0.213
8H-6, 100	67.91	68.50	04.50	*C. wuellerstorfi*	0.600	2.176			
8H-6, 120	68.01	68.61	04.50	*C. wuellerstorfi*	0.434	2.499	*G. margaritae*	0.350	–0.110
8H-7, 0	68.31	68.90	04.52	*C. wuellerstorfi*	0.549	2.265	*G. margaritae*	0.375	0.049
8H-7, 20	68.51	69.10	04.53	*C. wuellerstorfi*	0.208	2.522	*G. margaritae*	0.396	0.034
8H-7, 40	68.71	69.30	04.54	*C. wuellerstorfi*	0.640	2.416	*G. margaritae*	0.577	0.068
9H-1, 0	68.81	70.02	04.58	*C. wuellerstorfi*	0.691	2.267			
9H-1, 0	68.81	70.02	04.58	*C. wuellerstorfi*	0.253	2.477			
8H-7, 60	68.91	70.11	04.58	*C. wuellerstorfi*	0.778	2.289			
9H-1, 20	69.01	70.22	04.59	*C. wuellerstorfi*	0.509	2.127			
9H-1, 40	69.21	70.41	04.60	*C. wuellerstorfi*	0.156	2.580			
9H-1, 60	69.41	70.62	04.61	*C. wuellerstorfi*	0.360	2.618			
9H-1, 80	69.61	70.81	04.62	*C. wuellerstorfi*	0.571	2.594			
9H-1, 100	69.81	71.01	04.63	*C. wuellerstorfi*	0.546	2.080			
9H-1, 120	70.01	71.22	04.64	*C. wuellerstorfi*	0.622	2.029			
9H-1, 140	70.21	71.41	04.65	*C. wuellerstorfi*	0.571	2.305			
9H-2, 0	70.31	71.52	04.65	*C. wuellerstorfi*	0.286	2.781			
9H-2, 20	70.51	71.71	04.66	*C. wuellerstorfi*	0.343	2.353			
9H-2, 40	70.71	71.92	04.68	*C. wuellerstorfi*	0.402	2.252			
9H-2, 60	70.91	72.10	04.68	*C. wuellerstorfi*	0.804	2.109			
9H-2, 80	71.11	72.30	04.70	*C. wuellerstorfi*	0.280	2.354			
9H-2, 100	71.31	72.50	04.71	*C. wuellerstorfi*	0.409	2.279			
9H-2, 120	71.51	72.72	04.72	*C. wuellerstorfi*	0.239	2.315			
9H-2, 140	71.71	72.90	04.73	*C. wuellerstorfi*	0.416	2.122			
9H-3, 0	71.81	73.02	04.73	*C. wuellerstorfi*	0.525	2.048			
9H-3, 20	72.01	73.21	04.74	*C. wuellerstorfi*	0.293	2.195			
9H-3, 40	72.21	73.42	04.75	*C. wuellerstorfi*	0.564	2.158			
9H-3, 60	72.41	73.61	04.76	*C. wuellerstorfi*	0.453	2.144			
9H-3, 80	72.61	73.82	04.77	*C. wuellerstorfi*	0.576	2.109			
9H-3, 100	72.81	74.02	04.78	*C. wuellerstorfi*	0.391	2.110			
9H-3, 120	73.01	74.21	04.79	*C. wuellerstorfi*	0.313	2.401			
9H-3, 140	73.21	74.41	04.81	*C. wuellerstorfi*	0.549	1.949			
9H-4, 0	73.31	74.52	04.81	*C. wuellerstorfi*	0.670	2.013			
9H-4, 20	73.51	74.71	04.82	*C. wuellerstorfi*	0.428	1.950			
9H-4, 40	73.71	74.90	04.83	*C. wuellerstorfi*	0.532	1.888			
9H-4, 60	73.91	75.11	04.84	*C. wuellerstorfi*	0.170	2.295			
9H-4, 80	74.11	75.30	04.85	*C. wuellerstorfi*	0.202	2.231			
9H-4, 100	74.31	75.50	04.86	*C. wuellerstorfi*	0.606	1.920			
9H-4, 120	74.51	75.72	04.87	*C. wuellerstorfi*	0.547	1.921			

Table 1 (continued).

Core, section, interval (cm)	Depth (mbsf)	Composite depth (m)	Age (Ma)	Species	$\delta^{13}C$	$\delta^{18}O$	Species	$\delta^{13}C$	$\delta^{18}O$
159-959C-									
9H-4, 140	74.71	75.91	04.88	*C. wuellerstorfi*	0.423	1.992			
9H-5, 0	74.81	76.02	04.89	*C. wuellerstorfi*	0.094	2.301			
9H-5, 20	75.01	76.21	04.90	*C. wuellerstorfi*	0.377	2.316			
9H-5, 40	75.21	76.42	04.91	*C. wuellerstorfi*	0.712	2.131			
9H-5, 60	75.41	76.60	04.92	*C. wuellerstorfi*	0.543	2.114			
9H-5, 100	75.81	77.00	04.94	*C. wuellerstorfi*	0.563	2.067			
9H-5, 120	76.01	77.22	04.95	*C. wuellerstorfi*	0.575	2.158			
9H-5, 140	76.21	77.41	04.96	*C. wuellerstorfi*	0.594	1.934			
9H-6, 0	76.31	77.50	04.97	*C. wuellerstorfi*	0.154	2.032			
9H-6, 20	76.51	77.71	04.98	*C. wuellerstorfi*	0.129	2.305			
9H-6, 40	76.71	77.91	04.99	*C. wuellerstorfi*	0.656	2.288			
9H-6, 60	76.91	78.12	05.00	*C. wuellerstorfi*	0.691	2.178			
9H-6, 80	77.11	78.31	05.01	*C. wuellerstorfi*	0.715	2.021			
9H-6, 100	77.31	78.52	05.02	*C. wuellerstorfi*	0.507	2.422			
9H-6, 120	77.51	78.72	05.03	*C. wuellerstorfi*	0.546	2.329			
9H-6, 140	77.71	78.92	05.04	*C. wuellerstorfi*	0.735	2.176			
9H-7, 0	77.81	79.02	05.05	*C. wuellerstorfi*	0.625	2.238			
9H-7, 20	78.01	79.21	05.06	*C. wuellerstorfi*	0.673	2.150			
9H-7, 40	78.21	79.42	05.07	*C. wuellerstorfi*	0.707	2.245			
10H-1, 0	78.31	79.52	05.07	*C. wuellerstorfi*	0.110	2.399			
9H-7, 60	78.41	80.11	05.10	*C. wuellerstorfi*	0.753	2.156			
10H-1, 20	78.51	80.21	05.11	*C. wuellerstorfi*	0.634	2.141			
10H-1, 40	78.71	80.42	05.12	*C. wuellerstorfi*	0.812	2.258			
10H-1, 60	78.91	80.60	05.13	*C. wuellerstorfi*	0.819	2.146			
10H-1, 80	79.11	80.82	05.14	*C. wuellerstorfi*	0.685	2.217			
10H-1, 100	79.31	81.01	05.15	*C. wuellerstorfi*	0.767	2.099			
10H-1, 120	79.51	81.22	05.16	*C. wuellerstorfi*	0.821	2.175			
10H-1, 140	79.71	81.42	05.17	*C. pachyderma*	0.892	2.183			
10H-2, 0	79.81	81.52	05.18	*C. wuellerstorfi*	0.732	2.248			
10H-2, 20	80.01	81.71	05.19	*C. wuellerstorfi*	0.741	2.140			
10H-2, 60	80.41	82.10	05.21	*C. wuellerstorfi*	0.793	2.093			
10H-2, 80	80.61	82.30	05.22	*C. wuellerstorfi*	0.980	2.047			
10H-2, 100	80.81	82.52	05.24	*C. wuellerstorfi*	0.857	2.250			
10H-2, 120	81.01	82.71	05.25	*C. pachyderma*	0.256	2.379			
10H-2, 140	81.21	82.92	05.27	*C. wuellerstorfi*	0.795	2.512			
10H-3, 0	81.31	83.02	05.28	*C. wuellerstorfi*	0.607	2.260			
10H-3, 20	81.51	83.21	05.29	*C. wuellerstorfi*	0.619	2.128			
10H-3, 40	81.71	83.42	05.31	*C. wuellerstorfi*	0.577	2.387			
10H-3, 60	81.91	83.60	05.32	*C. pachyderma*	0.490	2.123			
10H-3, 80	82.11	83.82	05.33	*C. wuellerstorfi*	0.557	2.453			
10H-3, 100	82.31	84.02	05.35	*C. wuellerstorfi*	0.590	2.323			
10H-3, 120	82.51	84.21	05.36	*C. wuellerstorfi*	0.666	2.117			
10H-3, 140	82.71	84.42	05.38	*C. pachyderma*	0.512	1.887			
10H-4, 0	82.81	84.52	05.39	*C. wuellerstorfi*	0.789	2.166	*G. margaritae*	0.907	1.282
10H-4, 20	83.01	84.71	05.40	*C. wuellerstorfi*	0.930	2.106	*G. margaritae*	0.873	1.054
10H-4, 40	83.21	84.92	05.42	*C. wuellerstorfi*	0.824	2.155	*G. margaritae*	0.828	0.985
10H-4, 60	83.41	85.10	05.43	*C. wuellerstorfi*	1.248	2.280	*G. margaritae*	0.792	0.501
10H-4, 80	83.61	85.32	05.45	*C. wuellerstorfi*	0.990	2.063	*G. margaritae*	1.008	0.739
10H-4, 100	83.81	85.52	05.46	*C. wuellerstorfi*	0.855	2.185	*G. margaritae*	0.903	1.052
10H-4, 120	84.01	85.72	05.48				*G. margaritae*	0.579	1.103
10H-4, 140	84.21	85.91	05.49	*C. wuellerstorfi*	0.841	1.995	*G. margaritae*	0.715	0.810
10H-5, 0	84.31	86.01	05.50	*C. pachyderma*	0.715	1.982	*G. margaritae*	0.888	1.236
10H-5, 20	84.51	86.21	05.51	*C. wuellerstorfi*	0.593	2.299	*G. margaritae*	0.807	1.081
10H-5, 40	84.71	86.41	05.53	*C. wuellerstorfi*	0.399	2.164	*G. margaritae*	0.590	0.943
10H-5, 60	84.91	86.62	05.54	*C. wuellerstorfi*	0.417	2.625	*G. margaritae*	0.652	0.841
10H-5, 80	85.11	86.82	05.56	*C. wuellerstorfi*	0.719	2.210	*G. margaritae*	0.683	0.756
10H-5, 100	85.31	87.02	05.57	*C. wuellerstorfi*	0.754	2.436	*G. margaritae*	0.825	1.582
10H-5, 120	85.51	87.22	05.59	*C. wuellerstorfi*	0.546	2.498	*G. margaritae*	0.762	1.476
10H-5, 130	85.61	87.31	05.59	*C. wuellerstorfi*	0.503	2.658	*G. margaritae*	0.604	1.652
10H-5, 140	85.71	87.41	05.60	*C. wuellerstorfi*	0.413	2.677	*G. margaritae*	0.732	1.349
10H-6, 0	85.81	87.52	05.61	*C. wuellerstorfi*	0.781	2.479	*G. margaritae*	0.812	1.362
10H-6, 20	86.01	87.71	05.62	*C. wuellerstorfi*	1.024	2.308	*G. margaritae*	0.959	1.086
10H-6, 40	86.21	87.92	05.64	*C. pachyderma*	0.664	2.190	*G. margaritae*	0.769	1.084
10H-6, 60	86.41	88.10	05.66	*C. wuellerstorfi*	0.684	2.322	*G. margaritae*	0.719	1.081
10H-6, 80	86.61	88.32	05.68	*C. wuellerstorfi*	0.907	2.197			
10H-6, 100	86.81	88.52	05.69	*C. wuellerstorfi*	0.635	2.515			
10H-6, 120	87.01	88.72	05.71				*G. margaritae*	0.968	0.459
10H-6, 140	87.21	88.90	05.73	*C. wuellerstorfi*	0.740	2.302	*G. margaritae*	0.780	1.154
10H-7, 0	87.31	89.02	05.74	*C. wuellerstorfi*	0.674	2.384	*G. margaritae*	0.842	1.101
10H-7, 20	87.51	89.21	05.75	*C. wuellerstorfi*	0.993	2.237	*G. margaritae*	0.861	1.041
10H-7, 40	87.71	89.41	05.77	*C. wuellerstorfi*	0.950	2.293	*G. margaritae*	0.918	1.038
11H-1, 0	87.81	89.52	05.78	*C. pachyderma*	0.494	2.307	*G. margaritae*	0.721	0.893
10H-7, 60	87.91	90.82	05.89	*C. wuellerstorfi*	0.850	2.276	*G. margaritae*	0.752	0.795
11H-1, 20	88.01	90.91	05.89	*C. wuellerstorfi*	0.977	2.177	*G. margaritae*	0.675	0.827
11H-1, 40	88.21	91.12	05.91	*C. wuellerstorfi*	0.747	2.697	*G. margaritae*	0.636	0.869
11H-1, 60	88.41	91.31	05.93	*C. wuellerstorfi*	0.679	2.284			
11H-1, 100	88.81	91.71	05.96				*G. margaritae*	0.476	0.816
11H-1, 120	89.01	91.92	05.98	*C. wuellerstorfi*	0.611	2.512	*G. margaritae*	0.300	0.709
11H-1, 140	89.21	92.11	06.00	*C. wuellerstorfi*	0.337	2.590	*G. margaritae*	0.211	0.868
11H-2, 0	89.31	92.22	06.01	*C. wuellerstorfi*	0.675	2.374	*G. margaritae*	0.241	0.819
11H-2, 20	89.51	92.41	06.02				*G. margaritae*	0.397	0.660
11H-2, 40	89.71	92.62	06.04	*C. pachyderma*	0.599	2.284	*G. margaritae*	0.430	1.049
11H-2, 60	89.91	92.81	06.05	*C. wuellerstorfi*	0.588	2.124	*G. margaritae*	0.326	0.586
11H-2, 80	90.11	93.00	06.07	*C. wuellerstorfi*	0.783	2.358	*G. margaritae*	0.313	0.840
11H-2, 100	90.31	93.20	06.09	*C. wuellerstorfi*			*G. margaritae*	0.400	1.004
11H-2, 120	90.51	93.41	06.11	*C. wuellerstorfi*	0.800	2.050	*G. margaritae*	0.458	0.918
11H-2, 140	90.71	93.62	06.12	*C. wuellerstorfi*	0.612	2.370	*G. margaritae*	0.333	0.618
11H-3, 0	90.81	93.72	06.13	*C. pachyderma*	0.420	2.200	*G. margaritae*	0.263	1.048
11H-3, 40	91.21	94.12	06.17	*C. wuellerstorfi*	0.585	2.271	*G. margaritae*	0.134	0.417

Table 1 (continued).

Core, section, interval (cm)	Depth (mbsf)	Composite depth (m)	Age (Ma)	Species	$\delta^{13}C$	$\delta^{18}O$	Species	$\delta^{13}C$	$\delta^{18}O$
159-959C-									
11H-3, 60	91.41	94.30	06.18	*C. wuellerstorfi*	0.401	1.867	*G. cibaoensis*	0.014	0.353
11H-3, 80	91.61	94.52	06.20	*C. wuellerstorfi*	0.278	2.547	*G. margaritae*	–0.161	1.179
11H-3, 100	91.81	94.71	06.22	*C. wuellerstorfi*	0.432	2.135	*G. margaritae*	0.340	1.399
11H-3, 120	92.01	94.92	06.23	*C. wuellerstorfi*	0.527	2.224			
11H-3, 140	92.21	95.11	06.25	*C. wuellerstorfi*	0.841	2.054	*G. margaritae*	0.391	0.612
11H-4, 0	92.31	95.22	06.26	*C. wuellerstorfi*	0.545	2.140			
11H-4, 20	92.51	95.41	06.27	*C. wuellerstorfi*	0.629	2.206			
11H-4, 40	92.71	95.62	06.29	*C. wuellerstorfi*	0.629	2.366	*G. margaritae*	0.053	0.767
11H-4, 60	92.91	95.80	06.31	*C. wuellerstorfi*	0.843	2.208	*G. cibaoensis*	0.339	0.824
11H-4, 80	93.11	96.02	06.33	*C. wuellerstorfi*	0.981	2.156	*G. cibaoensis*	0.620	1.156
11H-4, 100	93.31	96.22	06.34	*C. wuellerstorfi*	0.788	2.261	*G. cibaoensis*	0.419	0.625
11H-4, 120	93.51	96.41	06.36	*C. wuellerstorfi*	0.329	2.214	*G. cibaoensis*	0.148	0.889
11H-4, 140	93.71	96.62	06.38	*C. wuellerstorfi*	0.586	2.175	*G. cibaoensis*	0.404	0.842
11H-5, 0	93.81	96.72	06.38	*C. wuellerstorfi*	0.581	2.050	*G. cibaoensis*	0.484	0.644
11H-5, 20	94.01	96.91	06.40	*C. wuellerstorfi*	0.626	2.387	*G. margaritae*	0.338	0.929
11H-5, 40	94.21	97.12	06.42	*C. wuellerstorfi*	0.558	2.323	*G. margaritae*	0.437	0.854
11H-5, 60	94.41	97.30	06.43	*C. wuellerstorfi*	0.605	2.302	*G. cibaoensis*	0.281	0.840
11H-5, 80	94.61	97.50	06.45	*C. wuellerstorfi*	0.974	2.189	*G. cibaoensis*	0.785	0.673
11H-5, 100	94.81	97.71	06.47	*C. wuellerstorfi*	1.062	2.156	*G. cibaoensis*	0.750	0.580
11H-5, 120	95.01	97.90	06.48	*C. wuellerstorfi*	0.725	2.114	*G. cibaoensis*	0.426	0.743
11H-5, 140	95.21	98.11	06.50	*C. wuellerstorfi*	0.225	2.386	*G. cibaoensis*	0.174	1.039
11H-6, 0	95.31	98.22	06.51	*C. wuellerstorfi*	0.716	2.179	*G. cibaoensis*	0.326	1.088
11H-6, 20	95.51	98.41	06.53	*C. wuellerstorfi*	0.930	2.069	*G. cibaoensis*	0.548	0.695
11H-6, 40	95.71	98.60	06.54	*C. wuellerstorfi*	1.054	2.048	*G. cibaoensis*	0.788	0.797
11H-6, 60	95.91	98.81	06.56	*C. wuellerstorfi*	0.652	2.248	*G. cibaoensis*	0.359	0.764
11H-6, 80	96.11	99.01	06.58	*C. wuellerstorfi*	0.559	2.581	*G. cibaoensis*	0.222	1.194
11H-6, 100	96.31	99.21	06.59	*C. wuellerstorfi*	0.546	2.226	*G. cibaoensis*	0.480	0.802
11H-6, 120	96.51	99.42	06.61	*C. wuellerstorfi*	1.037	2.306	*G. cibaoensis*	0.892	0.708
11H-6, 140	96.71	99.60	06.63	*C. wuellerstorfi*	0.843	2.273	*G. cibaoensis*	0.900	0.929
11H-7, 0	96.81	99.72	06.64	*C. wuellerstorfi*	0.789	2.116			
11H-7, 20	97.01	99.91	06.65	*C. wuellerstorfi*	0.821	2.376	*G. cibaoensis*	0.579	0.858
11H-7, 40	97.21	100.12	06.67	*C. wuellerstorfi*	0.650	2.070	*G. cibaoensis*	0.643	0.662
11H-7, 60	97.41	100.32	06.69	*C. wuellerstorfi*	0.568	2.302	*G. cibaoensis*	0.469	0.672

Table 2. Foraminifers from Atlantic core tops.

Core	Latitude	Longitude	Depth to thermocline base (m)	$\delta^{13}C$ *G. sacculifer*	$\delta^{18}O$ *G. sacculifer*	$\delta^{13}C$ *N. dutertrei*	$\delta^{18}O$ *N. dutertrei*
CH99-19-14 Pilot, 0-3 cm	8.15°S	17.4°E	150	1.768	–0.613	1.621	0.259
V29-144, 0-3 cm	0.12°S	6.3°W	80	1.551	–1.471	1.431	–0.056
CH99-11-10, 0-3.5 cm	2.04°N	20.44°W	80	1.964	–1.134	1.714	0.036
V27-180, 0-2 cm	3.33°N	21°W	80	2.079	–1.268	1.724	–0.307
V27-179, 0-2 cm	4.2°N	23.5°W	90	2.254	–1.107	1.705	–0.015
V22-190, 0-2 cm	6.03°N	21.26°W	80	1.992	–0.947	1.528	0.474
V30-45, 0-2 cm	6.3°N	19.933°W	75	2.052	–1.45	1.721	–0.351
V19-300, 0-2 cm	6.88°N	19.47°W	70	2.187	–0.833	1.687	0.298
V26-46, 0-2 cm	9.56°N	18.18°W	60	2.225	–0.998	1.649	0.112
V30-49, 4-5 cm	18.43°N	21.8°W	110	1.225	–0.986	1.717	–0.152
AII42-4-4PC, 0-2 cm	19.43°N	29.02°W	130	1.784	–0.527	1.518	0.387
V22-38, 2-4 cm	9.33°S	34.15°W	230	1.566	–1.202	1.876	–0.355
KNR110-43 PC, 1-3 cm	4.12°N	43.29°W	20	2.104	–1.445	2.036	–0.889
AII31-16-16 Pilot, 0-3 cm	11.95°N	46.16°W	160	1.913	–0.938	1.779	–0.398
CH75-18-16, 0-2 cm	13.38°N	43.87°W	180	1.736	–0.809	1.809	–0.176
CH75-7-5, 0-7 cm	14.24°N	58.41°W	210	1.599	–1.604	1.803	–0.801
CH75-6-4 PC, 0-8 cm	14.29°N	59.58°W	220	2.103	–1.431	1.503	–0.333
CH36-6-8 GC, 0-2 cm	16.58°N	57.91°W	200	1.712	–1.353	1.546	–0.504
AII42-15-14, 0-2 cm	19.34°N	44.57°W	170	1.292	–0.009	1.569	0.241

Note: CH = chain; AII = Atlantis II; V = Verna; KNR = Knorr.

secondary calcite. The dissolution of the chamber calcite should affect the chemistry of the whole shell since the chamber calcite is expected to have more negative $\delta^{18}O$ than crust calcite does, by analogy with globorotaliids. Hence, dissolution of chamber calcite should produce unusually positive $\delta^{18}O$ in *N. dutertrei* compared to the $\delta^{18}O$ of pristine specimens from the same sample. In contrast, *Globorotalia margaritae* is a thin-walled, dissolution-susceptible species that disappears in samples that contain high ratios of shell fragments. Consequently, the isotopic record of *G. margaritae* is unlikely to be biased strongly by partial solution because the shells are completely destroyed in dissolved samples. Therefore, analyses of *G. margaritae* were used to test whether the $\delta^{18}O$ variability in coexisting specimens of *N. dutertrei* might be due to partial dissolution of the shells.

Planktonic foraminifer $\delta^{13}C$ is commonly assumed to reflect ambient water chemistry, but there are several studies that question this. Many studies have noted a general correspondence between foraminifer $\delta^{13}C$ and the $\delta^{13}C$ of water that suggests that foraminifers can be used to reconstruct nutrient utilization and respiration in the upper water column. Fairbanks et al. (1982) showed that the $\delta^{13}C$ of *N. dutertrei, G. sacculifer,* and other species mirrors water column $\delta^{13}C$ in the Panama Basin. Studies of sediment traps and core tops have also found that foraminifer $\delta^{13}C$ is lowest in samples collected during upwelling times or under upwelling centers in many instances (Curry et al., 1992; Kroon and Ganssen, 1989; Sautter Reynolds and Thunell, 1991; Wefer et al., 1983) However, other studies have found a weak relationship between upwelling and foraminifer $\delta^{13}C$. For example,

Curry et al. (1983) found no obvious relationship between $\delta^{13}C$ and upwelling in near-surface growing species (*G. sacculifer* and *G. ruber*) collected in sediment traps from the Panama Basin. Likewise, Curry et al. (1992) found that although there was a distinct decrease in foraminifer $\delta^{13}C$ during peak upwelling in the Arabian Sea, there was not a significant change in foraminifer $\delta^{13}C$ along a transect from upwelling centers to non-upwelling regions. Finally, Ravelo and Fairbanks (1995) found no clear relationship between foraminifer $\delta^{13}C$ and depth habitat inferred from shell $\delta^{18}O$, despite the large vertical changes in water $\delta^{13}C$ from the surface mixed layer to thermocline waters. Hence, the utility of foraminifer $\delta^{13}C$ for deducing vertical hydrographic structure and upwelling remains an open problem.

RESULTS

Oxygen Isotope Trends

Planktonic foraminifer $\delta^{18}O$ records were roughly parallel in the late Miocene and early Pliocene with *G. sacculifer* ~2.0‰ more negative than coexisting *G. margaritae, G. cibaoensis,* and *N. dutertrei* (Fig. 4A) There was a modest trend toward more positive $\delta^{18}O$ in *G. sacculifer* between 6.7 and 5.9 Ma. The absence of a similar shift in benthic foraminifer $\delta^{18}O$ suggests that the trend in *G. sacculifer* $\delta^{18}O$ was not due to changes in $\delta^{18}O_{water}$ but reflected cooling of sea-surface temperature (SST) by ~2.3°C.

All planktonic foraminifer $\delta^{18}O$ records began to converge about 5.5 Ma. The absence of any major trend in $\delta^{18}O$ of benthic foraminifers again implies that variations in planktonic foraminifer $\delta^{18}O$ must have been largely due to changes in calcification temperature rather than ice volume. Some of the planktonic foraminiferal isotopic variation might also have been due to changes in surface ocean salinity, but the largest $\delta^{18}O$ shifts of >0.5‰ would have required salinity to change by more than 1‰—an unlikely event in this open ocean setting, far from major rivers.

At 4.9 Ma, $\delta^{18}O$ of *N. dutertrei* abruptly shifted to within 0.5‰ to 1‰ of *G. sacculifer.* The $\delta^{18}O$ gradient between *G. sacculifer* and *N. dutertrei* oscillated between 0.5‰ to 2.0‰ several times over the next one-half million years before permanently settling into a ~0.5‰ gradient between 4.3 Ma and the youngest part of the record at 3.5 Ma (Fig. 4A). The $\delta^{18}O$ of *G. margaritae* tracks that of *N. dutertrei* during the shift toward more negative $\delta^{18}O$ where we have overlapping records of these taxa between 4.3 and 4.6 Ma. The long-term $\delta^{18}O$ of *G. sacculifer* and *C. wuellerstorfi* did not change during these events, suggesting that the excursions represent abrupt changes in the temperature recorded by *N. dutertrei* and other thermocline-growing foraminifers.

Between 4.7 and 3.5 Ma, there was a distinct trend in $\delta^{18}O$ of *G. sacculifer* toward more positive ratios. The total increase was ~0.8‰ $\delta^{18}O$ and was accompanied by an increase in the amplitude of short oscillations in this record. As there was no corresponding long-term trend in the $\delta^{18}O$ of *N. dutertrei,* it is likely that the record of *G. sacculifer* indicates a general cooling of SST by ~3°–4°C with short period shifts of up to 5°C superimposed on this. Conversely, *Globorotalia crassaformis* displays a long-term decrease in $\delta^{18}O$ of ~1‰ between 4.25 and 3.5 Ma. Since the $\delta^{18}O$ of *G. crassaformis* is

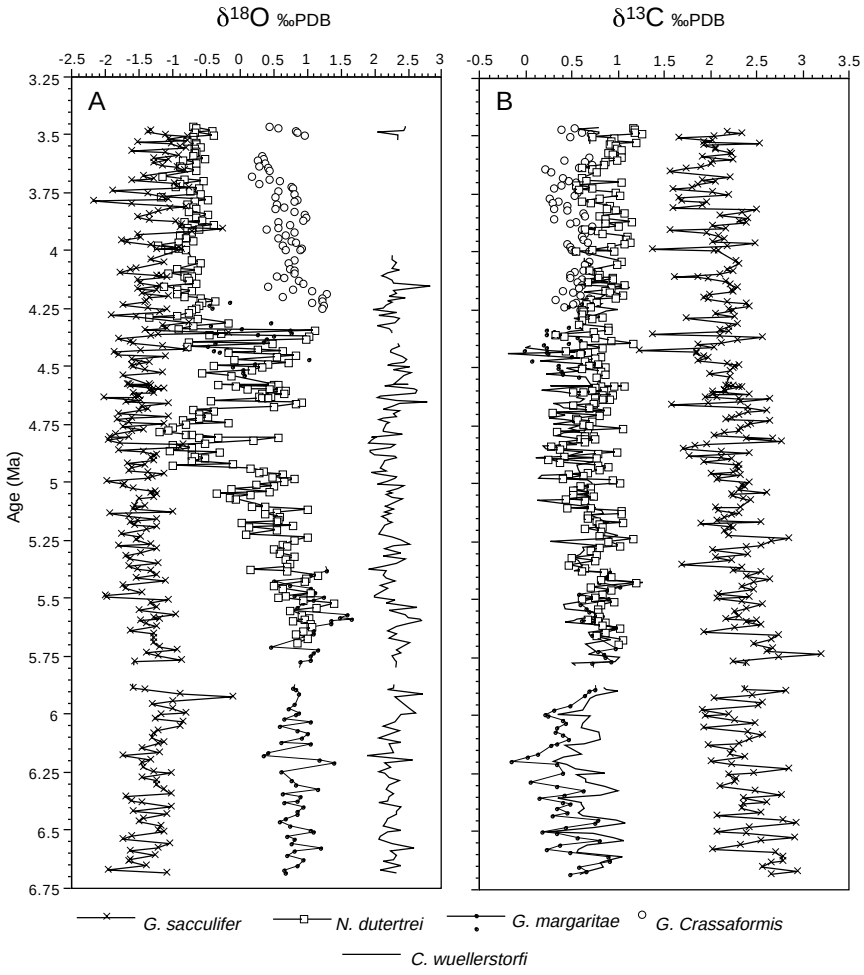

Figure 4. Stable isotope data plotted against an age scale based on composite depth, taking into account the amount of sediment not studied in core catchers or missing in core breaks. **A.** Records of $\delta^{18}O$ for species as in Figure 2. Records for *G. margaritae* shown as unconnected dots in the interval from 4.25 to 4.6 Ma for clarity. **B.** Records of $\delta^{13}C$ for the same species.

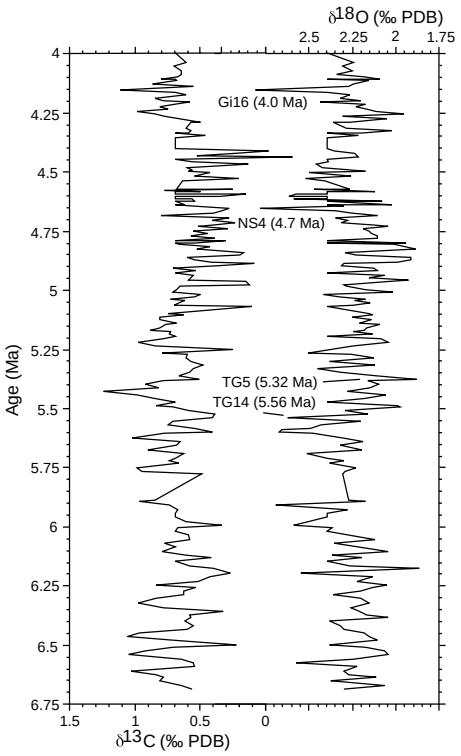

Figure 5. Detail of the stable isotope record for *C. wuellerstorfi* showing possible correlations to the isotope chronology of Shackleton et al. (1995).

believed to represent temperatures near the base of the thermocline, it appears that there was a general decrease in the strength of thermal gradient in the upper ocean due to both cooling of surface waters and warming of the deep thermocline.

The first appearance (FAD) of *G. crassaformis* is at 63.4 mbsf in Hole 959C (~4.27 Ma) and is about 230 k.y. younger than the evolutionary first appearance of this species at 4.5 Ma. The coincidence of the delayed FAD of *G. crassaformis* and the final collapse of the $\delta^{18}O$ gradient between *N. dutertrei* and *G. sacculifer* suggests that these events reflect a change in upper ocean hydrography. Notably, both the intervals of reduced *G. sacculifer-N. dutertrei* $\delta^{18}O$ gradient at ~4.35 and 4.75–4.9 Ma were associated with the rare occurrence of the typically cold-water species, *Neogloboquadrina pachyderma* (sinistral), for the only times at Site 959. The presence of *N. pachyderma* (s) is unusual since this species occurs most commonly south of the Polar Front. The occurrence of *N. pachyderma* (s) near the equator strongly suggests at least intermittent import of cool surface or thermocline waters into the Gulf of Guinea, perhaps through the Benguela Current or the Equatorial Undercurrent.

Dissolution Artifacts?

Overlapping records for *N. dutertrei* and *G. margaritae* are nearly coincident between 4.2 and 4.55 Ma and again between 5.4 and 5.75 Ma, suggesting that *G. margaritae* is a reasonable proxy for *N. dutertrei* before the first appearance of *N. dutertrei* at 5.75 Ma (Fig. 4A). Notably, the interval from 5.4 to 5.75 Ma falls within the Messinian desiccation event and coincides with moderate to poor preservation in foraminiferal assemblages. *G. margaritae* is a thin-walled dissolution-susceptible taxon, whereas *N. dutertrei* is susceptible to dissolution of the chamber interiors long before the shell is reduced to fragments. Therefore, the strong similarity between the $\delta^{18}O$ trends of *G. margaritae* and *N. dutertrei* in this time window suggest that their isotopic records are not strongly biased by dissolution.

Carbon Isotope Trends

Carbon isotopic ratios of *G. sacculifer* were 1‰ to 2‰ higher than those of other planktonic and benthic foraminifers (Fig. 4B). There was a long-term decline in the strength of this $\delta^{13}C$ gradient from a value of 2‰ to ~1.1‰ between 6.75 and 3.5 Ma produced by a large (~0.8‰) decrease in the $\delta^{13}C$ of *G. sacculifer* and a smaller (~0.3‰) increase in $\delta^{13}C$ of *N. dutertrei.*

The average value of benthic foraminiferal $\delta^{13}C$ did not change during the Pliocene. Instead, $\delta^{13}C$ of *C. wuellerstorfi* oscillated about a value of ~0.7‰ throughout the entire time series. The amplitude of benthic $\delta^{13}C$ variation was generally less than 0.5‰. Prominent intervals of positive benthic $\delta^{13}C$ occurred at ~5.4 and 4.2 Ma as well as a series of negative excursions near 4.43, 4.95, 5.07, 5.25, 5.55, and 6.01 Ma (Fig. 5). The timing of most of these benthic $\delta^{13}C$ events is close to that of a series of $\delta^{13}C$ shifts in the Pacific Ocean Drilling Program (ODP) Site 846 record (Shackleton et al., 1995) and raises the possibility that these may be of global significance.

Many of the major features of the benthic $\delta^{13}C$ record are replicated in $\delta^{13}C$ variations of *G. margaritae, N. dutertrei,* and *G. crassaformis.* The time series of *G. margaritae* and *G. cibaoensis* in the late Miocene reproduces the major features of the *C. wuellerstorfi* record including a prominent negative excursion at ~6.01 Ma just prior to a sharp increase in the $\delta^{13}C$ of all these species (Fig. 4B). *Globorotalia margaritae* $\delta^{13}C$ also displays a large negative excursion at ~4.43 Ma seen in the benthic record. In contrast, *N. dutertrei* appears only to preserve the long-term average $\delta^{13}C$ seen in benthic foraminifers, and damps out many of the short-period oscillations in the $\delta^{13}C$ of *C. wuellerstorfi* record.

A detailed comparison of the $\delta^{13}C$ histories of *G. sacculifer* and *N. dutertrei* (Fig. 6B) shows a rough parallelism of the records. The amplitude of $\delta^{13}C$ variability for *N. dutertrei* is less than half that of *G. sacculifer,* but many of the larger magnitude oscillations correlate between the two species. Likewise, the shifts toward negative $\delta^{13}C$ in the planktonic foraminifers were commonly associated with reductions in benthic foraminifer $\delta^{13}C$ (Fig. 4B), suggesting that changes in the oceanic $\delta^{13}C$ budget were partly responsible. In turn, most of the larger negative shifts in benthic $\delta^{13}C$ coincided with positive shifts in benthic $\delta^{18}O$, which suggests that the global $\delta^{13}C$ budget was modulated by glacial conditions similar to Pleistocene variations in oceanic $\delta^{13}C$. However, it is also possible, that some of the variability in $\delta^{13}C$ of *G. sacculifer* was due to changes in surface ocean hydrography since this species showed much larger oscillations in chemistry than thermocline and benthic species.

DISCUSSION

Hydrography and Relationship to the Surface Wind Field

Surface water circulation in the tropical Atlantic is largely a product of the position and strength of the Intertropical Convergence Zone (ITCZ) that migrates seasonally between 0° to 15°N over the eastern Atlantic (Fig. 7). The main surface currents are westward and include the North Equatorial Current at the southern edge of the North Atlantic Gyre, and its counterpart in the South Atlantic Gyre, the South Equatorial Current (SEC) (Peterson and Stramma, 1991; Richardson and McKee, 1984; Richardson and Philander, 1987). The SEC splits into two main systems on the eastern margin of Brazil with the main part of the flow crossing the equator to form the North Brazil Current that eventually flows into the Caribbean Sea while the remainder moves south along the coast (the Brazil Current). During the summer and fall, when the ITCZ moves well north of the equator,

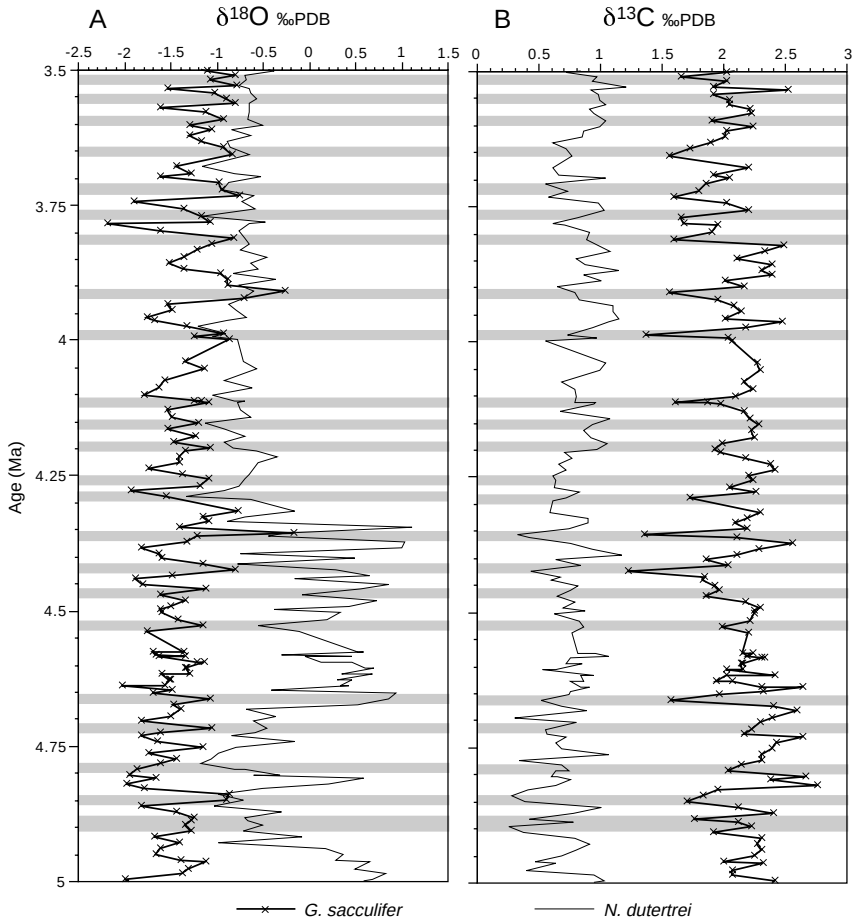

Figure 6. Detail of (**A**) $\delta^{18}O$ and (**B**) $\delta^{13}C$ time series of *G. sacculifer* and *N. dutertrei*. Shaded bands are intervals where the $\delta^{18}O$ of *G. sacculifer* is locally minimized and are thought to reflect drops in sea surface temperature related to upwelling.

warm surface waters piled against the Brazil margin by the SEC recirculate to the east to form the North Equatorial Countercurrent (NECC) that contributes to the east-flowing Guinea Current off western Africa (Fig. 7; Hastenrath and Merle, 1987; Peterson and Stramma, 1991; Richardson and McKee, 1984). The NECC weakens during boreal winter and spring when the ITCZ shifts to the south and westward-flowing surface winds oppose the eastward-flowing current (Fig. 7), whereas the Guinea Current flows eastward throughout the year as it is always located south of the ITCZ in an area of dominantly eastward-moving surface winds (Siedler et al., 1992).

Subsurface currents transport a considerable volume of water to the east below the westward flowing South Equatorial Current. The main eastward flow is concentrated in the Equatorial Undercurrent (EUC), part of which is deflected northward into the Gulf of Guinea (Peterson and Stramma, 1991; Siedler et al., 1992; Verstraete, 1992). The EUC carries cool, saline water from the South Atlantic and produces a particularly intense thermocline as it flows under the warm, relatively low salinity Guinea Current. Nonetheless, the strongest vertical temperature gradients are found in areas of strong divergence such as where the South Equatorial Current moves westward off the coast of Gabon, and is opposed at shallow depth by the eastward flowing EUC.

The strength of the thermocline in the Gulf of Guinea is closely related to wind stress over the western equatorial Atlantic. The EUC is strongest in the western equatorial Atlantic where it is formed by the pressure head developed as the trade winds pile warm surface waters against the Brazil margin (Peterson and Stramma, 1991). Only near the western boundary does the subsurface eastward pressure gradient exceed the frictional forces of the overlying westward surface currents, yielding an eastward flowing undercurrent. The undercurrent weakens as it moves east due to friction with overlying westward-flowing currents. Consequently, the strength of the EUC is very dependent upon the wind forcing in the western Atlantic. When the ITCZ moves south in the late winter and spring, and the strength of the trade winds drops, the EUC also weakens (Fig. 7; Peterson and Stramma, 1991; Verstraete, 1992).

Variations in wind strength in the western and central Atlantic have been proposed as playing a dominant role in the hydrography of the eastern tropical Atlantic somewhat analogous with the El Niño/Southern Oscillation (ENSO) phenomenon in the Pacific. During the Pacific ENSO, a southward shift in the ITCZ lowers the east-west zonal pressure gradient and strength of the trade winds along the equator. Gravity waves (Kelvin waves) are unleashed by the reduced pressure gradient and propagate eastward carrying warm surface water into the normally cool eastern Pacific. An analogous process occurs annually in the Atlantic when the ITCZ moves north in the boreal spring and summer and the increase in wind stress over the western Atlantic propagates Kelvin waves into the eastern Atlantic (Hastenrath and Merle, 1987; Peterson and Stramma, 1991). The gravity wave is reflected off the African continent and moves westward across the Gulf of Guinea producing regional upwelling along the coast (Peterson and Stramma, 1991; Verstraete, 1992). Thus, when the ITCZ moves northward, strengthening the countercurrent system, cool waters return to the Gulf of Guinea. Upwelling produced

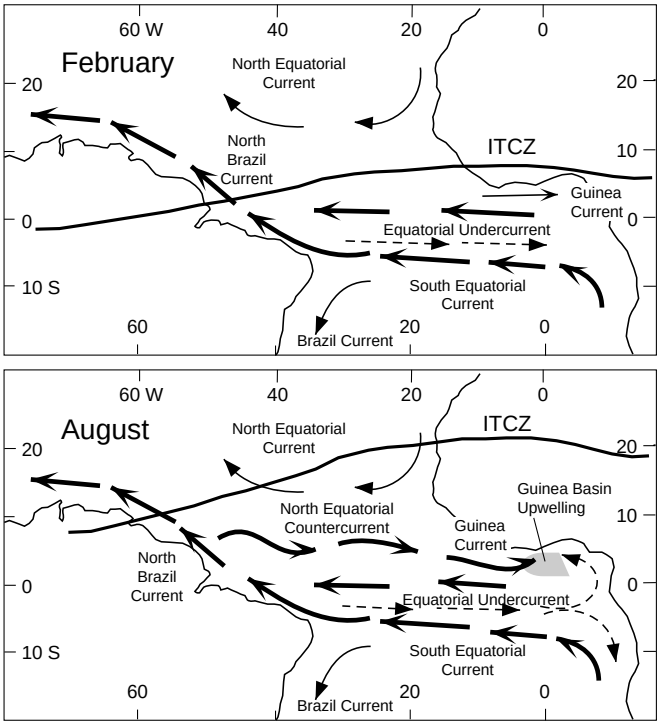

Figure 7. Maps of major currents in the equatorial Atlantic in relationship to the latitudinal position of the ITCZ (after Hastenrath and Merle, 1987).

by this system accounts for the peak carbonate fluxes observed in sediment traps from the northern Guinea Basin during boreal summer (Wefer and Fischer, 1993).

Years in which the ITCZ remains in a near equatorial position result in warm conditions over the entire tropical Atlantic. Upwelling is suppressed in the Gulf of Guinea and unusually warm waters penetrate into the northern Benguela Current system. An event like this occurred in the winter of 1984 following the most intense Pacific El Niño of this century (Peterson and Stramma, 1991; Verstraete, 1992). The thermocline flattened across the equatorial Atlantic and the 20°C isotherm reached a depth of 100 m in the eastern Atlantic—considerably deeper than the 20–50 m depth typical in this region. Heavy rains fell on equatorial and southwestern Africa breaking the droughts common during times when eastern Atlantic SSTs are cool. Hence, both the climatology of equatorial Africa and the thermocline structure of the eastern Atlantic are highly sensitive to wind strength over the western basins.

Hisard and Merle (1980) note that the Atlantic is generally characterized by warm surface waters compared to the eastern Pacific; in effect, El Niño conditions occur most of the time in the Atlantic and become extreme when the ordinary warm surface-water conditions are not broken by short upwelling events. In contrast, El Niños in the Pacific occur when the normal cool SSTs are interrupted by warm events. The size of the two oceans may play some role in this (Hisard and Merle, 1980). The small Atlantic Basin reacts quickly to seasonal forcing whereas the large Pacific Basin reacts more typically on an interannual time scale. A result is that the tropical Atlantic tends to have high annual variability in SST (~6°–8°C) because of the relatively extreme annual changes in the ITCZ position and heat budget of equatorial waters (Peterson and Stramma, 1991).

Planktonic Foraminifer Chemistry as a Proxy for Thermocline Structure

Several studies have shown that *G. sacculifer* calcifies largely in the surface mixed layer or very shallow thermocline while *N. dutertrei* grows in the thermocline (Curry et al., 1983; Fairbanks et al., 1982; Ravelo and Fairbanks, 1992; Ravelo and Shackleton, 1995; Sautter Reynolds and Thunell, 1991). Foraminifers caught in vertically stratified plankton tows yield $\delta^{18}O$ consistent with the water depths and temperatures from which they were collected (Fairbanks et al., 1982). Studies of planktonic foraminifers in sediment traps and core tops from the Panama Basin show a similar pattern (Curry et al., 1983; Kroon and Darling, 1995). A strong, stably stratified water column is present throughout the year and contributes to the ~2.0‰ $\delta^{18}O$ contrast between *G. sacculifer* and *N. dutertrei* seen throughout the year in sediment trap samples. Much the same is true for the eastern equatorial Atlantic, where the surface ocean has a strong, shallow thermocline throughout the year. There, the $\delta^{18}O$ gradient between *G. sacculifer* and *N. dutertrei* is about 1.5‰ (Ravelo and Fairbanks, 1992).

In contrast, regions with strong seasonal upwelling systems like the Arabian Sea and the upwelling centers off northwestern Africa produce much smaller $\delta^{18}O$ gradients between surface mixed-layer species and thermocline species. Monsoonal upwelling produces a very shallow and intense thermocline in the western Arabian Sea, which may account for the <0.5‰ $\delta^{18}O$ difference between mixed-layer taxa and thermocline species (Kroon and Darling, 1995; Kroon and Ganssen, 1989). Similarly, Ravelo and Fairbanks (1992) report a $\delta^{18}O$ difference of ~0.6‰–0.7‰ between *G. sacculifer* and *N. dutertrei* in a core from the northwest African upwelling center. Sediment traps in the Arabian Sea accumulate virtually all their particle and foraminiferal flux during upwelling periods (Curry et al., 1992). Hence it is perhaps not surprising that both mixed-layer taxa and thermocline taxa have similar $\delta^{18}O$ ratios since they all grow in the same upwelled water.

Comparison of the $\delta^{18}O$ of *G. sacculifer* and *N. dutertrei* from core tops in the tropical Atlantic shows that the isotopic gradient between these species mirrors the depth to the base of the thermocline (Fig. 8). In this figure the base of the thermocline is defined as the depth below which temperature changes by less than 2°C over a 50-m depth range (Hastenrath and Merle, 1987). Regions with a thick mixed layer and deep thermocline, like the western tropical Atlantic (Fig. 8B), have a $\delta^{18}O$ gradient between these species, which is about half that found in the eastern Atlantic (Fig. 8A). Where the $\delta^{18}O$ gradient is minimized in the northeastern basin, the thermocline is unusually shallow and reflects strong upwelling along the northwest African margin. Notably, surface-water temperatures are also depressed in the upwelling system. Both the deep thermocline of the western Atlantic and the strong upwelling region of the northeastern tropical Atlantic produce small $\delta^{18}O$ gradients in planktonic foraminifers but the upwelling system is associated with marked decrease in surface-water temperature while SST remains high in the deep-thermocline situation. In addition, these areas have completely different patterns of species dominance, as noted by Ravelo and Fairbanks (1992). *Neogloboquadrina dutertrei* is rare throughout most of the western tropical Atlantic in comparison with the eastern basin. Conversely, both *Globigerinoides ruber* and *G. sacculifer* dominate the assemblages in the western basins while these taxa are less abundant in the east.

There are few data on the depth habitats of *G. crassaformis* and *G. margaritae.* Existing data point to a deep-thermocline signature in *G. crassaformis* (e.g., Ravelo and Fairbanks, 1992) as this species has $\delta^{18}O$ more positive than all other species analyzed. Orr (1967) has shown that *G. crassaformis* apparently adds its "gametogenic" or

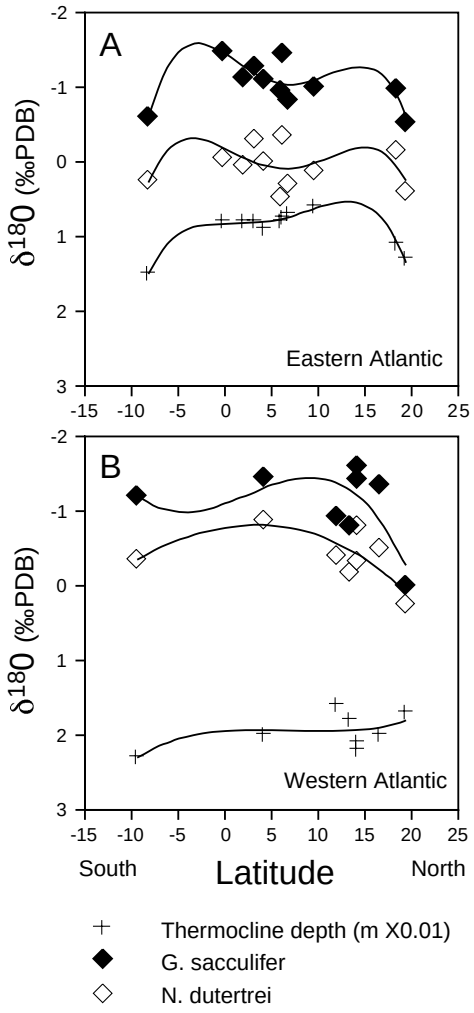

Figure 8. Gradients of $\delta^{18}O$ between *G. sacculifer* and *N. dutertrei* in north-south transects of core tops from the (**A)** eastern Atlantic and (**B**) western Atlantic. Note the similarity of the $\delta^{18}O$ gradient to the depth of the thermocline. Thermocline depth is estimated from the February map of thermocline depth of Hastenrath and Merle (1987). Measurements of both species are based on >10 specimens per analysis with both taxa selected from the 300- to 355-µm sieve fraction, and the data are presented in Table 2.

secondary calcite crust, at a greater depth than other globorotaliids, based on an analysis of the depths at which the majority of individual specimens are crusted in a transect of core tops across the shelf and upper slope in the Gulf of Mexico. *Globorotalia margaritae* has not been the subject of many stable isotope studies. However, this species appears to have a $\delta^{18}O$ signature similar to that of *N. dutertrei* in this study. Norris et al. (unpubl. data) found that *G. margaritae* has more negative $\delta^{18}O$ than all other coexisting species of lower Pliocene globorotaliids at Deep Sea Drilling Project Hole 516A on the Rio Grande Rise in the South Atlantic.

History of Thermocline Depth in the Gulf of Guinea

During the late Miocene to earliest Pliocene, a large (>2‰) difference in $\delta^{18}O$ between the mixed-layer species, *G. sacculifer,* and thermocline species, *G. margaritae* and *N. dutertrei,* suggests that the Gulf of Guinea was well stratified. The modern Panama Basin may represent an analog. There, upwelled waters do not typically reach into the surface mixed layer so the surface waters remain warm all year round. The pronounced thermal gradient of ~12°–14°C in the Panamanian thermocline is consistent with 1.8‰ to 2‰ difference between *G. sacculifer* and *N. dutertrei* in the Pliocene Gulf of Guinea. The modern eastern equatorial Atlantic off of Gabon has a similar hydrography as shown by Ravelo and Fairbanks (1992; see also Fig. 9).

About 5.2 Ma, the temperature gradient in the upper thermocline gradually decreased as shown by a long-term reduction in the $\delta^{18}O$ contrast between *N. dutertrei* and *G. sacculifer* (Fig. 4A). The amplitude of temperature variability in the thermocline also appears to have increased as suggested by glacial-interglacial scale shifts of up to 1‰ in the $\delta^{18}O$ of *N. dutertrei.* A reduced surface-to-thermocline temperature gradient suggests a decrease in surface ocean stratification, perhaps associated with a more seasonal thermocline or with a drop in coastal divergence. The glacial-interglacial variability in temperature and $\delta^{18}O_{water}$ was small at this time and can account for no more than half of the increased amplitude of temperature variation in the thermocline.

There was a precipitous drop in thermocline stratification about 4.92 Ma in which the $\delta^{18}O$ difference between the uppermost thermocline and the middle thermocline shrank to ~0.5‰ (Fig. 6A). The decrease in $\delta^{18}O$ gradient from 2.0‰ to 0.5‰ is consistent with a drop in the temperature difference across the middle to upper thermocline of as much as ~7°C, nearly all of which was accommodated by warming of the middle thermocline in the habitat range of *N. dutertrei. Neogloboquadrina dutertrei* was common to abundant throughout this time as expected if the mixed layer remained shallow and the Gulf of Guinea continued to be influenced by upwelling. The maintenance of upwelling in the area is also supported by the presence of *N. pachyderma* (s). The abundance of *N. dutertrei* and *N. pachyderma* (s) as well as the small $\delta^{18}O$ gradient between *G. sacculifer* and *N. dutertrei* are all consistent with establishment of a more weakly stratified water column like that present in the modern Gulf of Guinea than had existed earlier in the Pliocene.

This change in thermal gradient can be accommodated almost entirely by changes in the thermocline rather than the depth of the mixed layer. An example is offered by the contrast between the extremely sharp thermocline in the South Equatorial Current off the coast of modern Gabon and the thermocline in the modern Gulf of Guinea (Fig. 9). The surface mixed layer is of similar depth in both regions, but the thermoclines have different slopes. The temperature gradient in the upper 30 m is about 7°C off Gabon, but less than 2°C in the Gulf of Guinea. Therefore, much of the decreased $\delta^{18}O$ gradient observed at 4.9 Ma at Site 959 could be produced by a change in the gradient of the thermocline analogous to a change from the thermal structure of the modern South Equatorial Current to that of the Guinea Current.

An alternative interpretation is that the change in $\delta^{18}O$ gradient between planktonic foraminifer at 4.9 Ma reflects an expansion of the surface mixed layer like that reflected in the contrast in $\delta^{18}O$ gradient between the eastern and western Atlantic (Fig. 8). Indeed, there is no pronounced drop in surface-water temperature that might be expected with a change to a very strong upwelling system like that off of modern North Africa, suggesting that the drop in $\delta^{18}O$ gradient cannot be due to the onset of unusually strong upwelling in the Gulf of Guinea. Yet, the presence of *N. pachyderma* (s) and the abundance of *N. dutertrei* both suggest that the surface waters did not become as oligotrophic as those of the modern western Atlantic. In addition, it is hard to understand how a deep mixed layer could be maintained in the eastern Atlantic where the modern mixed layer varies from 10 to 20 m deep in areas of divergence like the South Equatorial Current to 20 to 30 m deep in areas of convergence like the Guinea Current (Hastenrath and Merle, 1987). Hence, if a change in mixed-layer depth is partly responsible for the variation in planktonic foramin-

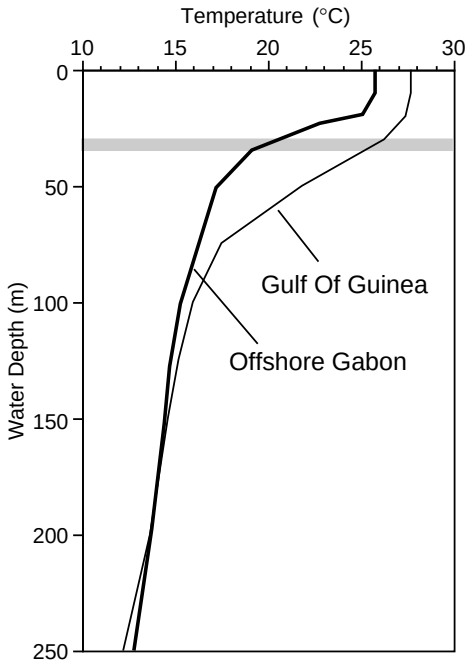

Figure 9. Average seasonal thermal gradients in the upper ocean for the southern Gulf of Guinea and the South Equatorial Current (SEC) off Gabon. The SEC has a very strong thermocline compared to the Guinea Current in the Gulf of Guinea, but both areas have similar mixed-layer depths. Note that the temperature gradient between the surface and 30 m (stippled band) is about 2° to 2.5°C in the Gulf of Guinea, but more than 7°C in the SEC. The thermocline weakens seasonally in both areas to produce regional upwelling. Data for Gabon station from Hisard and Merle (1980; fig. 5) and Verstraete (1992; 4°W section, fig. 10) for Gulf of Guinea Station.

iferal $\delta^{18}O$ gradient, the adjustment in mixed-layer depth must have been a subtle one. Possibly, small changes in both mixed-layer depth and thermocline gradient are responsible for the abrupt decrease in the planktonic foraminiferal $\delta^{18}O$ gradient with both sets of hydrographic changes reflecting the establishment of the Guinea Current about 4.9 Ma.

About 4.68 Ma, the thermocline apparently strengthened, as indicated by re-establishment of a $\delta^{18}O$ gradient of ~2‰ between *G. sacculifer* and *N. dutertrei*, and briefly returned to the extremely sharp, strong thermocline like the one that existed before ~4.9 Ma. However, this hydrographic structure was not stable on a glacial-interglacial time scale because the $\delta^{18}O$ of *N. dutertrei* went through large oscillations that suggest major changes in the depth or strength of the thermocline.

At 4.33 Ma, the hydrography of the Gulf of Guinea switched back to the more gentle thermocline structure that had existed intermittently since 4.92 Ma. The absence of large oscillations in $\delta^{18}O$ gradient between the mixed layer and the middle thermocline suggests that there were few major changes in thermocline structure between 4.33 Ma and the youngest part of the isotopic record at 3.5 Ma. An increase in the amplitude of *G. sacculifer* $\delta^{18}O$ starting about 4.75 Ma suggests that SST became more variable and may reflect an increase in the strength or duration of upwelling.

Indeed, there is a pronounced isotopic signal of upwelling from at least 5 Ma to the top of the record at 3.5 Ma. Repeatedly, the $\delta^{18}O$ gradient in the thermocline was minimized, even in periods when the $\delta^{18}O$ gradient was large (e.g., 5.1–4.9 Ma and 4.68–4.33 Ma). Many of the decreases in thermocline strength are associated with sharp decreases in the $\delta^{13}C$ of *G. sacculifer* (Fig. 6B). These decreases in $\delta^{13}C$ probably reflect changes in the carbon isotope budget of the oceans, like those associated with glacial stages in the Pleistocene, and suggest that the episodes of most intense upwelling occurred during glacial periods. It is unclear whether the $\delta^{13}C$ shifts directly reflect upwelling since there is contradictory evidence for a direct control of water column CO_2 on the $\delta^{13}C$ of living foraminifers (see above). However, the amplitude of $\delta^{13}C$ in *G. sacculifer* is about twice that of co-existing thermocline and benthic species, which suggests that part of the isotopic signal in *G. sacculifer* may reflect either local hydrography or a greater physiological sensitivity to $\delta^{13}C$ variations due to the presence of algal symbionts.

Trade Wind Strength and History of ITCZ Migration

Reconstructions of the position of the ITCZ in the late Miocene and early Pliocene place this front in a relatively northern position compared with today in both the Pacific and the Atlantic (Hay and Brock, 1992; Pisias et al., 1995). Both stable isotope and carbonate accumulation data suggest that winds over the central and eastern tropical Pacific were more zonal than today (summarized by Pisias, 1995). Hay and Brock (1992) speculated that the northern position of the ITCZ was due in part to an expansion of glaciers on Antarctica that pushed the South Atlantic Subtropical High to the north and displaced the ITCZ, as well. These authors also note that the combination of a more northerly ITCZ and southerly position of the east-west–trending Guinea Coast of Africa (at ~2.5°N at 5 Ma compared to ~5°N today) would have prevented the EUC from entering the Gulf of Guinea. Instead, the Gulf of Guinea would have been within the central part of the South Equatorial Current and would have had a strong, shallow thermocline, such as is present off the Angolan and Gabon coasts today. The strong $\delta^{18}O$ gradient in the thermocline at Site 959 before ~5 Ma is consistent with this scenario.

A strong thermocline in the Gulf of Guinea during the early Pliocene and late Miocene is difficult to assign to any single cause. The desiccation of the Mediterranean has been suggested as a means of displacing the ITCZ far to the north by enlarging the area of warm landmass at middle latitudes (e.g., Hay and Brock, 1992). However, the Messinian crisis falls within a prolonged period of strong thermal gradients in the Gulf of Guinea, suggesting that the desiccation event either had no effect on the position of the ITCZ, or the trade winds remained sufficiently far to the north before and after the crisis that they failed to affect the hydrography of the easternmost Atlantic. Likewise, it is difficult to determine at what point the northward drift of Africa would have finally allowed countercurrents to penetrate the Gulf of Guinea.

The establishment of the Guinea Current at ~4.92 Ma suggests that Africa had drifted sufficiently far to the north that the North Equatorial Counter Current (NECC) could penetrate the Gulf of Guinea. Likewise, the ITCZ had begun to seasonally move far enough south to form the NECC and send Kelvin waves into the eastern equatorial Atlantic. In the Pacific, analysis of eolian sediments also suggests a southward shift of the ITCZ to <7°N between 4 and 5 Ma (Hovan, 1995; Pisias et al., 1995). The subsequent strengthening of the thermocline in the Gulf of Guinea at ~4.68 Ma is evidence for a return to a somewhat more northerly position of the ITCZ, but the oscillations in thermocline gradient between 4.33 and 4.68 Ma suggest that countercurrents and Kelvin waves did reach the Gulf periodically during this time. Finally, the apparently permanent presence of the Guinea Current in the Gulf at 4.33 Ma, may reflect the establishment of the modern seasonal migration cycle of the ITCZ.

The summer position of the ITCZ, when it is in its most northerly location, seems not to have changed substantially over the past 4 m.y., based upon studies of dust outbreaks along the northwestern African margin (Tiedemann et al., 1989). Their evidence is contrary

to the opinion of Hay and Brock (1992) who suggested that the ITCZ should have remained in a northerly position until the establishment of Northern Hemisphere glaciation at ~3.4 Ma when the increase in Northern Hemisphere meridional temperature gradient would have displaced the ITCZ south to its near its present location.

Implications for the West African Monsoon

Modeling studies (Prell and Kutzbach, 1987) and paleoclimatic evidence from India and Africa (Kutzbach and Street-Perrott, 1985; Rossignol-Strick, 1983; Ruddiman et al., 1989; Tiedemann et al., 1994) suggest that continental aridity maxima are associated with minimum summer insolation levels that reduce the strength of summer monsoons. Over the southern Sahara, weakened monsoons should be associated with increases in airborne dust as vegetation dies off. The strength of the West African Monsoon is related to the land-sea temperature contrast such that cooler SST results in a weakened monsoon. This relationship between the monsoon and SST is indicated by climatological and hydrographic studies in which El Niño conditions of unusual warming of the eastern Atlantic are associated with unusually strong rainfall over coastal west Africa (Verstraete, 1992).

Hence, we might expect that periods of intense upwelling in the Gulf of Guinea should be associated with a weakened monsoon and greater aridity over the Sahel in sub-Saharan Africa. In effect, upwelling periods with minimal SST should be in phase with insolation minima and with intervals of increased dust flux. Uncertainties in the time scale for Hole 959C prevent a direct comparison with existing dust flux records. Yet, the correlation between glacial stages suggested by lows in *G. sacculifer* $\delta^{13}C$ and upwelling stages in the Gulf of Guinea implied by short reductions in the planktonic foraminiferal $\delta^{18}O$ gradient suggest that there may be a good correlation with periods of Northern Hemisphere insolation minima. More generally, the periods when there was a strong, shallow thermocline in the Gulf of Guinea (4.33–4.68 Ma and >4.9 Ma) may correlate with relatively humid periods over the Sahel, since these are times of some of the warmest SSTs recorded in the Hole 959C record. Indeed, dust fluxes were generally low between ~4.3–7 Ma (Tiedemann et al., 1989) corresponding approximately with the period when a strong, shallow thermocline existed in the Gulf of Guinea.

Ruddiman et al. (1989) and Kutzbach et al. (1989) have noted that uplift of the Tibetan Plateau may be the ultimate arbiter of African aridity both through proximate changes in the zonal moisture gradient over the Sahel and through modification of atmospheric circulation over the Sahara. In this respect, changes in SST and upwelling strength in the eastern Atlantic are probably an effect of changes in atmospheric forcing rather than an ultimate cause of aridification.

CONCLUSIONS

Stable isotope records have been constructed for several species of planktonic foraminifers and the benthic species, *C. wuellerstorfi* for the upper Miocene to lower Pliocene at Site 959 with a moderate sample interval of ~10–12 k.y. Oxygen isotopic gradients between the mixed layer, or shallow thermocline species *G. sacculifer* and the middle thermocline species *G. margaritae, G. cibaoensis,* and *N. dutertrei* show that the thermocline was shallow and well stratified from the latest Miocene until ~4.92 Ma. Observations of $\delta^{18}O$ gradients between modern *G. sacculifer* and *N. dutertrei* in sediment trap samples and core tops support the interpretation that large $\delta^{18}O$ differences between species are associated with strong, permanent thermoclines such as exist today in the tropical eastern Pacific and eastern Atlantic. About 4.9 Ma, the thermocline weakened in the Gulf of Guinea, which probably reflects the initiation of the Guinea Current. The shift from a very strongly stratified water column before 4.9 Ma to a slightly deeper and weaker thermocline is probably related to a southward shift in the position of the ITCZ that introduced the North Equatorial Counter Current and Kelvin waves into the Gulf of Guinea for the first time. The northward drift of Africa may also have played a role in the timing of formation of the Guinea Current through gradual displacement of the east-west–trending coast of West Africa into the Northern Hemisphere. The establishment of the Guinea Current in the Gulf of Guinea evidently precedes the initiation of Northern Hemisphere glaciation by more than 2 m.y. and suggests that the southward movement of the ITCZ during the early Pliocene was not the result of cooling in the Arctic. Southward displacement of the ITCZ may be partly responsible for expansion of African aridity in the early Pliocene by disrupting the warm, strongly stratified waters of the Gulf of Guinea and weakening the West African Monsoon. However, it is probable that cooling of the Gulf of Guinea is but a link in the chain of events leading to aridification of Saharan Africa with more ultimate causes, like the uplift of the Tibetan Plateau, playing an important role as well through modification of global atmospheric circulation.

ACKNOWLEDGMENTS

I thank Tom Wagner and the Ocean Drilling Program for supplying the samples analyzed here and Lu Ping Zou for help in washing, picking, and preparing foraminifers for stable isotope analysis. The manuscript benefited greatly from reviews by Christina Ravelo and Paul Pearson. Thanks also to JOI/USSAC and the Ocean Drilling Program for financial support of this research and participation in the scientific party on Leg 159.

REFERENCES

Berger, W.H., Killingley, J.S., and Vincent, E., 1978. Stable isotopes in deep-sea carbonates: box cores ERDC-92, west equatorial Pacific. *Oceanol. Acta,* 1:203–216.

Berggren, W.A., Hilgen, F.J., Langereis, C.G., Kent, D.V., Obradovich, J.D., Raffi, I., Raymo, M.E., and Shackleton, N.J., 1995. Late Neogene chronology: new perspectives in high-resolution stratigraphy. *Geol. Soc. Am. Bull.,* 107:1272–1287.

Curry, W.B., Ostermann, D.R., Guptha, M.V.S., and Ittekkot, V., 1992. Foraminiferal production and monsoonal upwelling in the Arabian Sea: evidence from sediment traps. *In* Summerhayes, C.P., Prell, W.L., and Emeis, K.C. (Eds.), *Upwelling Systems: Evolution Since the Early Miocene.* Geol. Soc. Spec. Publ. London, 93–106.

Curry, W.B., Thunell, R.C., and Honjo, S., 1983. Seasonal changes in the isotopic composition of planktonic foraminifera collected in Panama Basin sediment traps. *Earth Planet. Sci. Lett.,* 64:33–43.

Duplessy, J.-C., Blanc, P.-L., and Bé, A.W.H., 1981a. Oxygen and carbon isotopic composition and biogeographic distribution of planktonic foraminifera in the Indian Ocean. *Palaeogeogr., Palaeoclimatol., Palaeoecol.,* 33:9–46.

————, 1981b. Oxygen-18 enrichment of planktonic foraminifera due to gametogenic calcification below the euphotic zone. *Science,* 213:1247–1250.

Erez, J., 1978. Vital effect on stable-isotope composition seen in foraminifera and coral skeletons. *Nature,* 273:199–202.

Erez, J., and Honjo, S., 1981. Comparison of isotopic composition of planktonic foraminifera in plankton tows, sediment traps and sediments. *Palaeogeogr., Palaeoclimatol., Palaeoecol.,* 33:129–156.

Fairbanks, R.G., Sverdlove, M., Free, R., Wiebe, P.H., and Bé, A.W.H., 1982. Vertical distribution and isotopic fractionation of living planktonic foraminifera from the Panama Basin. *Nature,* 298:841–844.

Hastenrath, S., and Merle, J., 1987. Annual cycle of subsurface thermal structure in the tropical Atlantic Ocean. *J. Phys. Oceanogr.,* 17:1518–1538.

Hay, W.W., and Brock, J.C., 1992. Temporal variation in intensity of upwelling off southwest Africa. *In* Summerhayes, C.P., Prell, W.L., and Emis, K.C. (Eds.), *Upwelling Systems: Evolution Since the Early Miocene.* Geol. Soc. Spec. Publ. London, 463–497.

Hisard, P., and Merle, J., 1980, Onset of summer surface cooling in the Gulf of Guinea during GATE. *Deep-Sea Res., Suppl. II,* 26:325−341.

Hovan, S.A., 1995. Late Cenozoic atmospheric circulation intensity and climatic history recorded by eolian deposition in the eastern equatorial Pacific Ocean, Leg 138. *In* Pisias, N.G., Mayer, L.A., Janecek, T.R., Palmer-Julson, A., and van Andel, T.H. (Eds.), *Proc. ODP., Sci. Results,* 138: College Station, TX (Ocean Drilling Program), 615−625.

Kroon, D., and Darling, K., 1995. Size and upwelling control of the stable isotope composition of *Neogloboquadrina dutertrei* (d'Orbigny), *Globigerinoides ruber* (d'Orbigny) and *Globigerina bulloides* d'Orbigny: examples from the Panama Basin and Arabian Sea. *J. Foraminiferal Res.*, 25:39−52.

Kroon, D., and Ganssen, G., 1989. Northern Indian Ocean upwelling cells and the stable isotope composition of living planktonic foraminifers. *Deep-Sea Res. Part A,* 36:1219−1236.

Kutzbach, J.E., Guetter, P.J., Ruddiman, W.F., and Prell, W.L., 1989. Sensitivity of climate to late Cenozoic uplift in southern Asia and the American west: numerical experiments. *J. Geophys. Res.*, 94:18393−18407.

Kutzbach, J.E., and Street-Perrott, F.A., 1985. Milankovitch forcing of fluctuations in the level of tropical lakes from 18 to zero kyrBP. *Nature,* 317:130−134.

Lohmann, G.P., 1995. A model of variation in the chemistry of planktonic foraminifers due to secondary calcification and selective dissolution. *Paleoceanography,* 10:445−458.

Norris, R.D., 1995. Reproductive ecology and stable isotope signature in planktic foraminifera. *ICP V Progr. Abstr.,* 56.

Orr, W.N., 1967. Secondary calcification in the foraminiferal genus *Globorotalia. Science,* 157:1554−1555.

Peterson, R.G., and Stramma, L., 1991. Upper-level circulation in the South Atlantic Ocean. *Progr. Oceanogr.,* 26:1−73.

Pisias, N.G., Mayer, L.A., and Mix, A.C., 1995. Paleoceanography of the eastern equatorial Pacific during the Neogene: synthesis of Leg 138 drilling results. *In* Pisias, N.G., Mayer, L.A., Janecek, T.R., Palmer-Julson, A., and van Andel, T.H. (Eds.), *Proc. ODP, Sci. Results,* 138: College Station, TX (Ocean Drilling Program), 5−21.

Prell, W.L., and Kutzbach, J.E., 1987. Monsoon variability over the past 150,000 years. *J. Geophys. Res.,* 92:8411−8425.

Ravelo, A.C., and Fairbanks, R.G., 1992. Oxygen isotopic composition of multiple species of planktonic foraminifera: recorders of the modern photic zone temperature gradient. *Paleoceanography,* 7:815−831.

————, 1995. Carbon isotopic fractionation in multiple species of planktonic foraminifera from core-tops in the tropical Atlantic. *J. Foraminiferal Res.,* 25:53−74.

Ravelo, A.C., and Shackleton, N.J., 1995. Evidence for surface-water circulation changes at Site 851 in the eastern tropical Pacific Ocean. *In* Pisias, N.G., Mayer, L.A., Janecek, T.R., Palmer-Julson, A., and van Andel, T.H. (Eds.), *Proc. ODP, Sci. Results,* 138: College Station, TX (Ocean Drilling Program), 503−514.

Richardson, P.L., and McKee, T.K., 1984. Average seasonal variation of the Atlantic equatorial currents from historical ship drifts. *J. Phys. Oceanogr.,* 14:1226−1238.

Richardson, P.L., and Philander, S.G.H., 1987. The seasonal variations of surface currents in the tropical Atlantic Ocean: a comparison of ship drift data with results from a general circulation model. *J. Geophys. Res.*, 92:715−724.

Rossignol-Strick, M., 1983. African monsoons: an immediate climate response to orbital insolation. *Nature,* 304:46−49.

Ruddiman, W.F., Sarnthein, M., Backman, J., Baldauf, J.G., Curry, W., Dupont, L.M., Janecek, T., Pokras, E.M., Raymo, M.E., Stabell, B., Stein, R., and Tiedemann, R., 1989. Late Miocene to Pleistocene evolution of climate in Africa and the low-latitude Atlantic: overview of Leg 108 results. *In* Ruddiman, W., Sarnthein, M., et al., *Proc. ODP, Sci. Results,* 108: College Station, TX (Ocean Drilling Program), 463−484.

Sautter Reynolds, L.R., and Thunell, R., 1991. Seasonal variability in the $\delta^{18}O$ and $\delta^{13}C$ of planktonic foraminifera from an upwelling environment: sediment trap results from the San Pedro Basin, Southern California Bight. *Paleoceanography,* 6:307−334.

Schweitzer, P.N., and Lohmann, G.P., 1991. Ontogeny and habitat of modern menardiiform planktonic foraminifera. *J. Foraminiferal Res.,* 21:332–346.

Shackleton, N.J., Hall, M.A., and Pate, D., 1995. Pliocene stable isotope stratigraphy of Site 846. *In* Pisias, N.G., Mayer, L.A., Janecek, T.R., Palmer-Julson, A., and van Andel, T.H. (Eds.), *Proc. ODP, Sci. Results,* 138: College Station, TX (Ocean Drilling Program), 337−355.

Siedler, G., Zangenberg, N., Onken, R., and Morliére, A., 1992. Seasonal changes in the tropical Atlantic circulation: observation and simulation of the Guinea Dome. *J. Geophys. Res.*, 97: 703−715.

Spero, H.J., and DeNiro, M.J., 1987. The influence of symbiont photosynthesis on the $\delta^{18}O$ and $\delta^{13}C$ values of planktonic foraminiferal shell calcite. *Symbiosis,* 4:213−228.

Spero, H.J., Lerche, I., and Williams, D.F., 1991. Opening the carbon isotope "vital effect" black box; 2: quantitative model for interpreting foraminiferal carbon isotope data. *Paleoceanography,* 6:639–655.

Tiedemann, R., Sarnthein, M., and Shackleton, N.J., 1994. Astronomic timescale for the Pliocene Atlantic $\delta^{18}O$ and dust flux records of Ocean Drilling Program Site 659. *Paleoceanography,* 9:619−638.

Tiedemann, R., Sarnthein, M., and Stein, R., 1989. Climatic changes in the western Sahara: aeolo-marine sediment record of the last 8 million years (Sites 657−661). *In* Ruddiman, W., Sarnthein, M., et al., *Proc. ODP, Sci. Results,* 108: College Station, TX (Ocean Drilling Program), 241−277.

Verstraete, J.-M., 1992. The seasonal upwellings in the Gulf of Guinea. *Progr. Oceanogr.,* 29:1−60.

Wefer, G., Dunbar, P.B., and Suess, E., 1983. Stable isotopes of foraminifers off Peru recording high fertility and changes in upwelling history. *In* Thiede, J., and Suess, E. (Eds.), *Coastal Upwelling: Its Sediment Record* (Pt. B): New York (Plenum), 295–308.

Wefer, G., and Fischer, G., 1993. Seasonal patterns of vertical particle flux in equatorial and coastal upwelling areas of the eastern Atlantic. *Deep-Sea Res.,* 40:1613–1645.

Date of initial receipt: 16 September 1996
Date of acceptance: 30 April 1997
Ms 159SR-021